Synthesis and characterization of GaP quantum dots and their application as color converters in LEDs

Changhoon Choi

Department of Chemical Engineering
Graduate School of UNIST

2015

Synthesis and characterization of GaP quantum dots and their application as color converters in LEDs

A thesis
submitted to the Graduate School of UNIST
in partial fulfillment of the
requirements for the degree of
Master of Science

Changhoon Choi

12. 19. 2014 Month/Day/year of Submission
Approved by

_____

Major Advisor
Jongnam Park

Synthesis and characterization of GaP quantum dots and their application as color converters in LEDs

Changhoon Choi

This certifies that the thesis of Changhoon Choi is approved.

12. 19. 2014 Month/Day/year of Submission

Signature

Thesis supervisor: Jongnam Park

Signature

Name of Thesis Committee Member: Kyoung Jin Choi

Signature

Name of Thesis Committee Member: Tae-Hyuk Kwon

Abstract

The semiconductor nanomaterials have received substantial interest in the last 20 years due to the great chemical, physical properties of them. The initial studies of this field were actively conducted about containing cadmium (Cd) and lead (Pb) group II-VI semiconductors because these nanomaterials can be easily obtained by the control of nucleation and growth steps via various synthetic methods such as the hot injection method, or heating-up process. Also, these materials have tried to be used for the various applications such as LEDs, solar cell, color conversion devices, and drug delivery. However, despite the excellent optical and chemical properties of group II-VI quantum dots (QDs), applications of group II-VI nanomaterials are limited due to the toxicity of cadmium and lead. There are active researches to solve these problems through the development of synthetic methods for the non-toxic group III-V nanomaterials. However, the studies were just focused on indium phosphide (InP) nanocrystals and the materials to replace group II-V nanomaterials still lack. In this study, we presented the first results of colloidal gallium phosphide (GaP) QDs synthesis with remarkable optical properties for applying optical devices. The colloidal GaP QDs were synthesized by using the appropriate combination of precursors. The emission wavelengths of GaP QDs were mainly controlled from 400 nm to 520 nm by the ratio of precursors to surfactants. Moreover GaP QDs presented photoluminescence quantum yield (PL QY) of 35~40% and FWHM of ~75 nm in green emission. Furthermore, the GaP QDs with green emission (520 nm) were applied as color conversion materials in color conversion device with UV LED and blue LED chips. As a result, we obtained green emission by color conversion of GaP QDs and the average color conversion efficiencies were calculated in 10~15%. The performance of devices still lacked to use single color conversion materials but that was sufficient to confirm the possibility of GaP QDs as next generation color conversion materials.

Blank page

Table of Contents

List of figures

List of tables

Nomenclature

QD	Quantum Dots
PL	Photoluminescence
EL	Electroluminescence
XRD	X-ray diffraction analysis
QY	Quantum Yield
CCE	Color Conversion Efficiency
LED	Light Emitting Diodes
TEM	Transmission Electron Microscope
FWHM	Full width at half maximum

Chapter 1
Introduction and Motivation

1.1 Introduction and motivation

Nanomaterials have received especial attentions in the last few decades because of their interesting optical, chemical, magnetic, electronic, and catalytic properties that cannot be achieved by bulk matarials.[1] Many researchers had been trying to apply these unique properties for many technological applications. Especially, nanomaterials have two representative properties for many applications. First, nanomaterials have dramatic increase in ratio of surface to volume when size of materials is reduced to nanometer scale (figure 1.1). For this reason, Nanomaterials can make new reaction not possible with bulk materials. Second, quantum confinement effect can be observed in nanomaterials whose diameter is smaller than the size of exciton Bohr radius. This property has often been utilized in semiconductor nanomaterials. Because the size of semiconductor nanomaterials is decreased below exciton Bohr radius, We can easily control their band gaps and apply various applications such as quantum dot Light emitting diodes(QD-LED)[2], QD color converters[3], and QD solar cells[4] (figure 1.2). Since the 2000s, the researchers who have verified potential of nanomaterials started the active study of nanomaterials using diverse synthesis methods such as sol-gel, electro spinning, hydrothermal, and colloidal methods. As a result of these studies we can apply nanomaterials for energy storage system, bio application, catalyst, and optoelectronic devices (Figure 1.3).

Specially, research of colloidal synthesis for nanomaterials has been becoming very important on use of many applications. Because we not only have synthesized nanomaterials such as nanoparticles[5], nanowires[6], and nanorods[7] simply by colloidal synthesis but also needed inexpensive initial cost for setting vacuum line. In addition, we can observe the properties change by size difference and a better performance can be expected in various applications because the synthesis of nanomaterials using colloidal method can be obtained a uniform sized and shape than other synthesis method. In previous studies of monodisperse nanomaterials the researchers published synthesis of 6~13 nm iron oxide nanoparticles in 1 nm increment controls in the magnetic nanoparticle fields[8]. In addition, band gaps of Cadmium based semiconductor materials can be controlled from 1.4 eV to 2.5 eV covering entire visible wavelength by changing synthesis condition simply and then these materials applied full color quantum dot LEDs[9] and energy transfer devices-WLED (Figure 1.4). Especially, Semiconductor nanoparticles needed high crystallinity, narrow band gap, and no defect sites for high performance of

device that can be satisfied by colloidal synthesis. Also, Colloidal synthesis is divided in two parts of methods, heat-up method and hot injection method (Figure 1.5). In heat-up method, all precursors and surfactant is mixed before heating up for reaction temperature. The T. Hyeon group pioneered the heat-up method to synthesize monodisperse metal, metal oxide nanoparticles[5]. In hot injection method, organometallic compounds were generally injected at high temperature (=nucleation temperature) in hot metal-surfactant complexes solution then temperature were reduced compared to nucleation temperature for growth of nanoparticles. The Bawendi group pioneered[10] the hot injection method and have developed the method to synthesis various type semiconductor nanoparticles.

In this dissertation, facile hot-injection method of new III-V semiconductor nanoparticles has developed and has suggested possibility of optical applications using these materials.

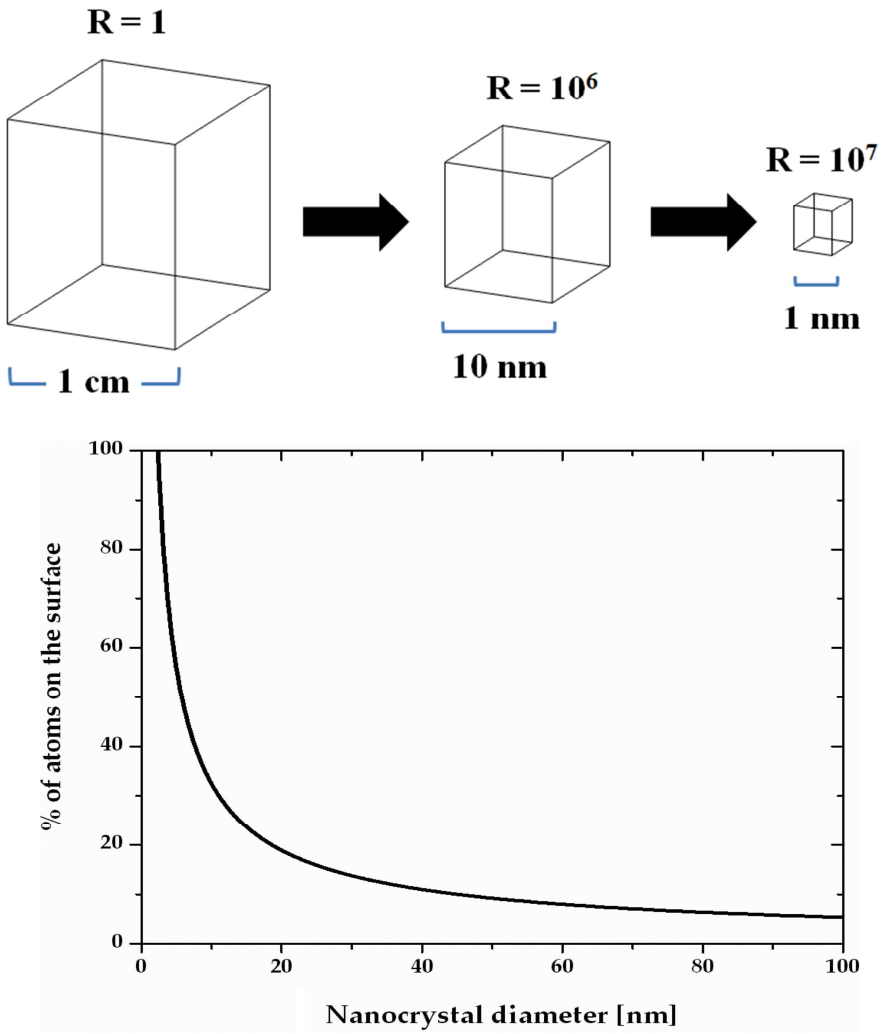

Figure 1.1 Ratio of surface atoms to interior atoms/ approximate percentage of surface atoms on PbS nanoparticles

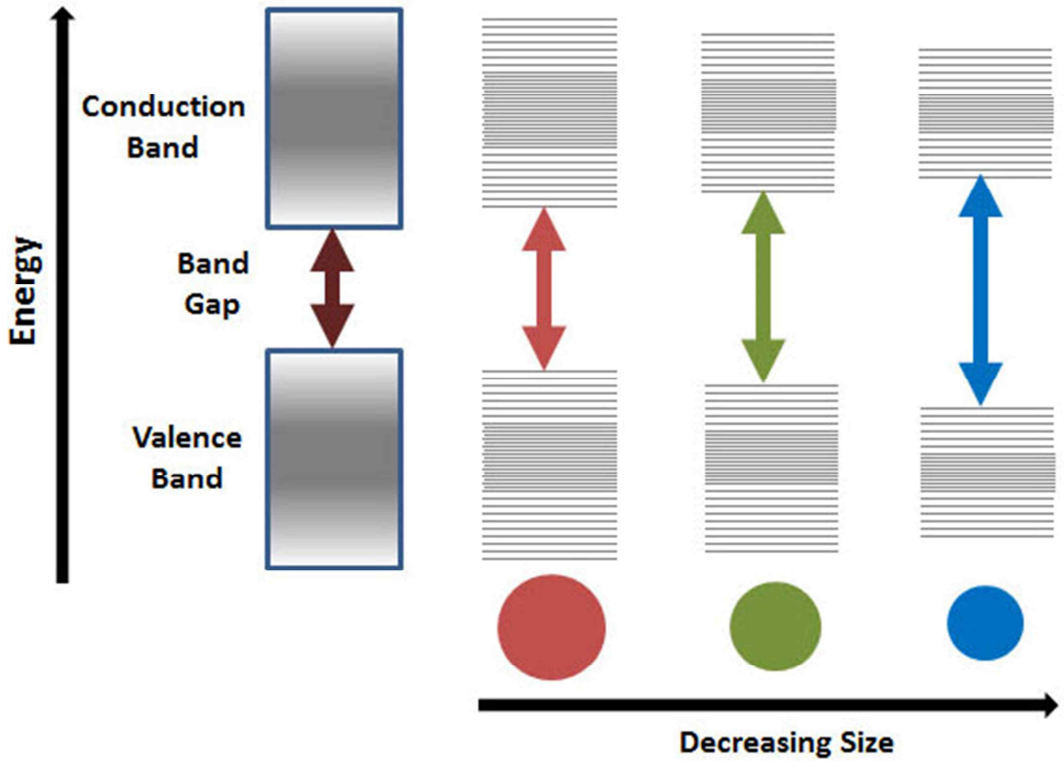

Figure 1.2 Concept of quantum confinement effect

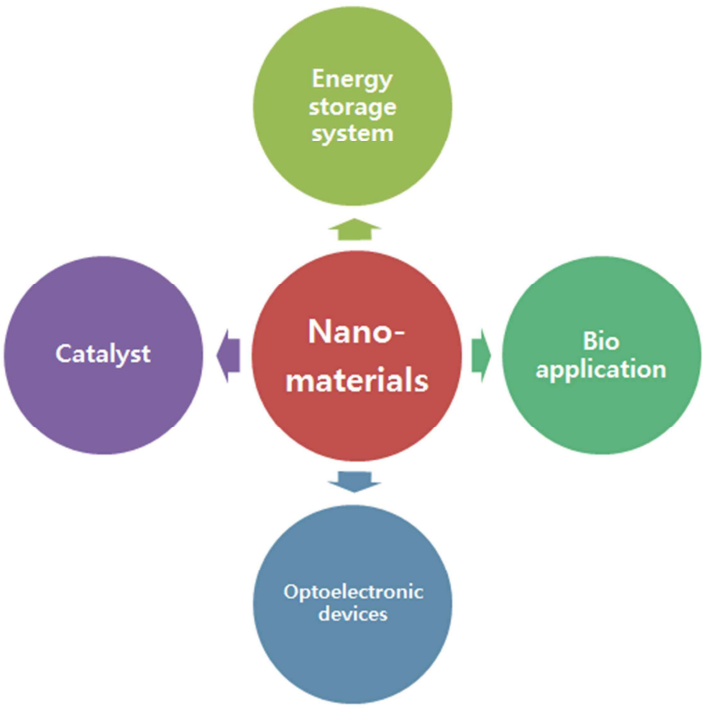

Figure 1.3 Schematic illustrations of examples of practical application by nanomaterials

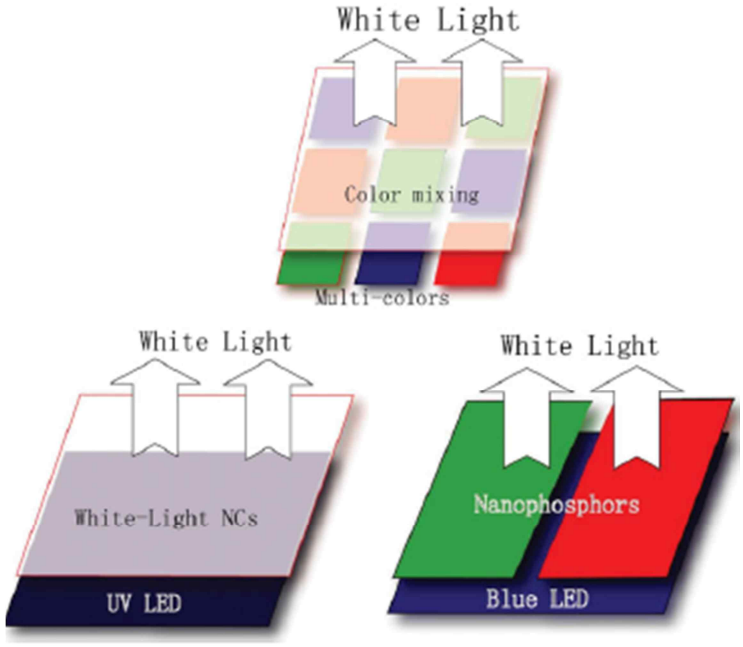

Figure 1.4 Various types of energy transfer light emitting devices (WLED)[11]

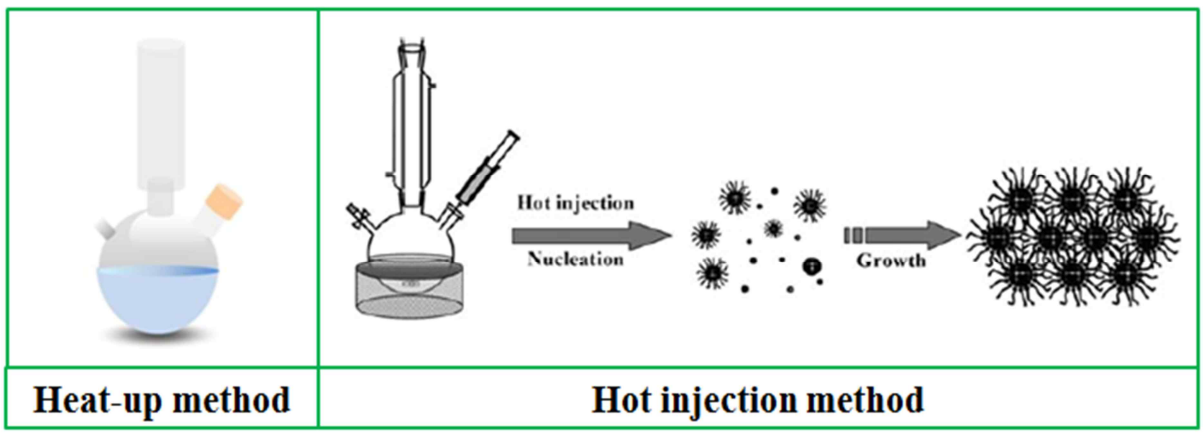

Figure 1.5 Scheme of heat-up method and hot injection method[1]

1.2 Colloidal semiconductor nanoparticles (Quantum dots)

Colloidal semiconductor nanoparticles, also termed "quantum dots" (QD), are composed of inorganic cores made by a few hundred ~ a few thousand atoms and organic outer layers of surfactant molecules (ligands) surrounding inorganic cores. Their small nano-size results in a quantum confinement effect that is defined by an increasing band gaps by the quantization of the energy levels to discrete values. Initial research of Quantum dots was focused on Cadmium based materials such as CdSe, CdTe, and CdS. In the first study of QD, the researchers used dimethyl cadmium (Me_2Cd), organometallic compound, and TOP-E (E=S, SE, TE TOP= trioctylphosphine) to synthesize Cadmium based Semiconductor nanomaterials in Bawendi group in 1993[10]. Nevertheless the Concept of solvent and surfactant were not properly separated, precursors used in that study have been widely used even now because of excellent reactivity of them. After Bawendi's report in 1993, a lot of researchers have studied synthesis of simple quantum dot core, as well as, a variety of synthesis techniques such as core-shell structure, alloy QD, metal doped QD, and shape control. I briefly introduce QD synthesis techniques to investigate the research trends.

1.2.1 Core-shell structure

The nanometric particle size results in a very high surface to volume ratio. Then these particles of high population of surface atoms partially compose of complex formation with the stabilizing ligands such as TOP, fatty acid. Nevertheless a critical fraction of organically passivated core QDs generally exhibit surface related deep trap states working as fast non-radiative recombination routes, thereby reducing PL QY, and making broad emission peak. To solve this limit point of only core QDs, the core-shell structure have been adopted in study field of quantum dots. The basic concept of core- shell structure is making inorganic shell on the surface of pre-synthesized semiconductor nanomaterials (core) with the result that non-radiative recombination by surface defects is reduced. Especially, control of shell thickness control is an important point in the fabrication of Core-shell structure. Provided the shell is very thin, passivation of nanomaterial (core) is not effective, resulting in reduced stability in the part of optical properties such as absorbance, PL, and QY. In inverse case, strain induces by lattice mismatch between core and shell materials and new defect sites are generated. As a result, optical properties of too thick core-shell structure quantum dots are generally deteriorated. When the researchers design core-shell structure, they have considered very important points (lattice mismatch and band gap). As mentioned above, the first important point is lattice mismatch (Table1.1). Lattice mismatch between core and shell materials is small, the growth of shell on core surface is easier then shell thickness can be controlled by synthesis condition. The second important point is

band gap. The core shell structure is divided by typical 3 types of core-shell structure. Figure 1.6 represents an overview of conduction band and valence band alignment of bulk semiconductor materials used in core-shell structure quantum dots. The three cases of core-shell structure can be defined and demonstrated type I, type II, and reverse type I (The upper part of figure 1.7).

In the type I, the band gap of shell materials is larger than that of core materials and both electron and hole are confined in the core so type I shell is used to passivate surface of core with purpose to improve optical properties of QDs. In other words, type I shells can separate surface of optically active core form QD's surrounding medium such as oxygen and water. So type I structure has used optical devices such as LED[12], color conversion device[13], and bio-imaging[14].

In the type II, valence band or conduction band edge of shell material is located in band gap of core. The researchers have usually applied the type II QD to QD solar cell. Because Shell growth leads to a smaller effective band gap and red shift of QD emission, that is favorable to solar cell. The typical examples are CdTe@CdSe and CdSe@ZnTe[15].

In the reverse type I, the band gap of shell materials is smaller than that of core materials then electrons and holes are confined in the shell depending on thickness of the shell. (Ex: CdS@HgS[16], CdS@ CdSe[17], etc.)

The core-shell structure is mostly synthesized by two step synthesis. Pre-synthesis of core quantum dots follows by a purification step, and shell growth steps. During shell growth step, in order to prevent nucleation of shell materials and fabricate 1~5 monolayers of shell materials on the surface of core, shell growth temperature is generally lower than core synthesis temperature. Moreover, a syringe pump is used at shell growth step to add shell precursors slowly (Figure 1.8). Nowadays we can synthesize core-shell structure without intermediate purification steps, and syringe pump, then we can calculate the required amount of shell precursors to fabricate suitable shell thickness. As a result, one of the developed synthesis method for core-shell structure is SILAR (successive ion layer adsorption and reaction) method[18] (Figure 1.8). This method is based on fabrication of a monolayer at a time by alternating inaction of anionic and cationic precursors.

The research on core-shell structure has been developed in the direction that makes more convenient synthesis method of core-shell structure such as one-pot synthesis. For example, Bae et al. published single-step synthesis of CdSe@gradient shell (Cd, Zn, Se, and S) using difference of reactivity of precursors[19]. These days this approach has been published for a variety of semiconductor materials as well as CdSe.

Material	Structure [300K]	Type	E_{gap} [eV]	Lattice parameter [Å]	Density [kg m^{-3}]
ZnS	Zinc blende	II–VI	3.61	5.41	4090
ZnSe	Zinc blende	II–VI	2.69	5.668	5266
ZnTe	Zinc blende	II–VI	2.39	6.104	5636
CdS	Wurtzite	II–VI	2.49	4.136/6.714	4820
CdSe	Wurtzite	II–VI	1.74	4.3/7.01	5810
CdTe	Zinc blende	II–VI	1.43	6.482	5870
GaN	Wurtzite	III–V	3.44	3.188/5.185	6095
GaP	Zinc-blende	III–V	2.27	5.45	4138
GaAs	Zinc blende	III–V	1.42	5.653	5318
GaSb	Zinc blende	III–V	0.75	6.096	5614
InN	Wurtzite	III–V	0.8	3.545/5.703	6810
InP	Zinc blende	III–V	1.35	5.869	4787
InAs	Zinc blende	III–V	0.35	6.058	5667
InSb	Zinc blende	III–V	0.23	6.479	5774
PbS	Rocksalt	IV–VI	0.41	5.936	7597
PbSe	Rocksalt	IV–VI	0.28	6.117	8260
PbTe	Rocksalt	IV–VI	0.31	6.462	8219

Table 1.1 Various materials parameters of bulk semiconductors[20]

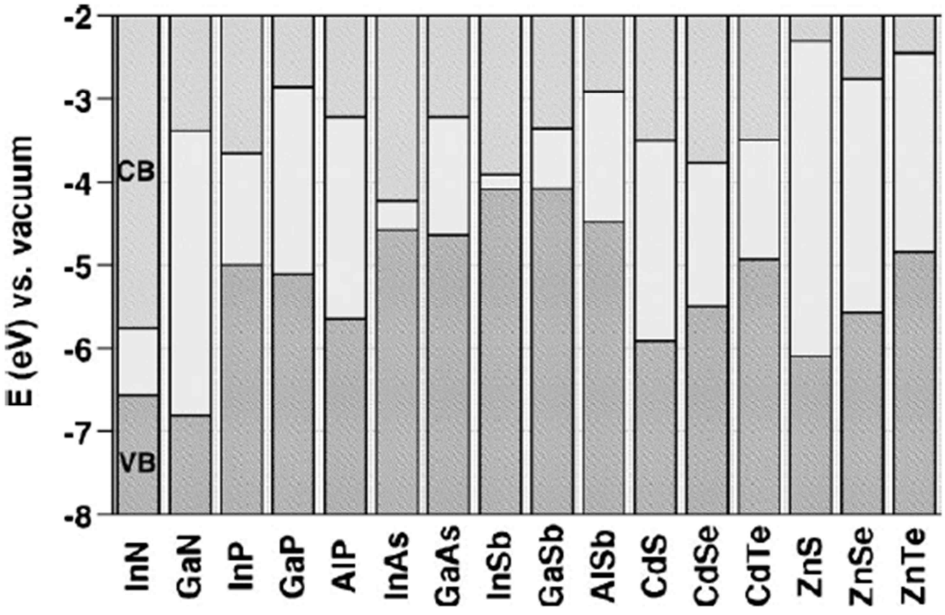

Figure 1.6 Electronic energy levels of various semiconductors[20]

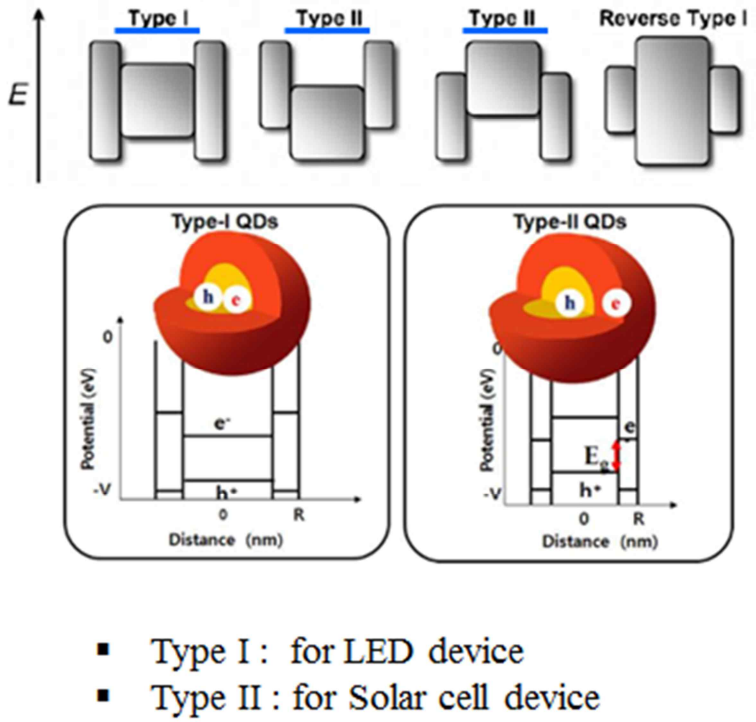

- Type I : for LED device
- Type II : for Solar cell device

Figure 1.7 3 Types of core-shell structure[20] / scheme of electrons and holes movement in type I,II

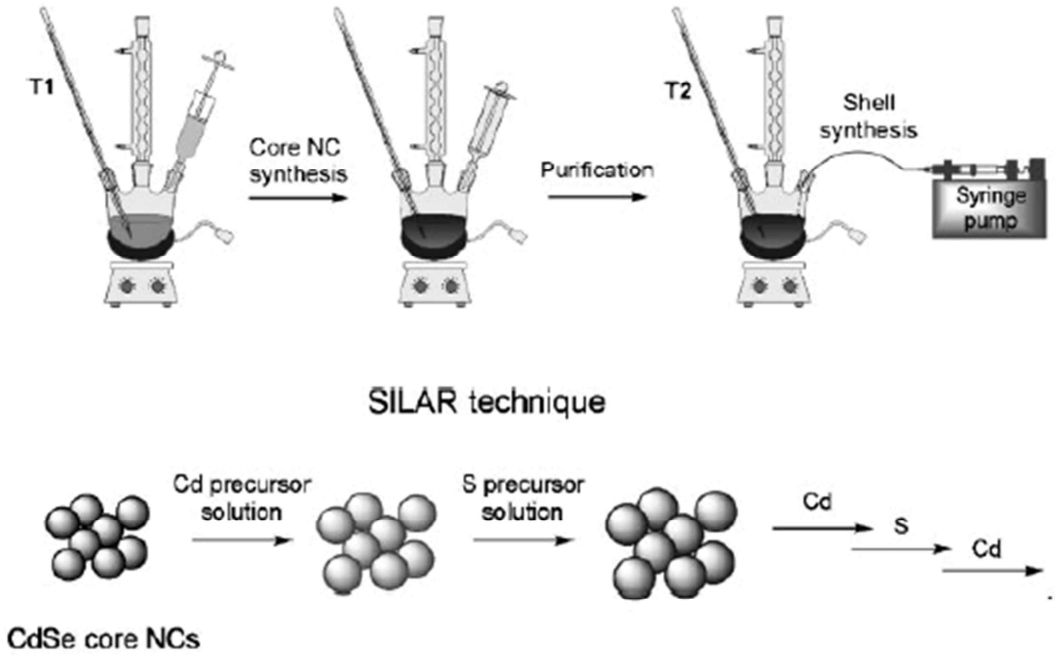

Figure 1.8 Scheme of two step synthesis and SILAR method[20]

1.2.2 Cd-free quantum dots

A group of II-VI semiconductor nanoparticles, for example, CdSe quantum dots, exhibit a tunable emission wavelength, high quantum yield (QY), and batter photo-stability than organic phosphors[14]. However, CdSe QDs have limited various applications for commercialization due to toxicity and low acceptability of Cadmium based materials. To solve these problems, InP quantum dot, one of the III-V group quantum dots, are the most desirable alternative that can offer optical properties similar to that of CdSe quantum dots (Table 1.2). Of course, there are many candidates to alternate CdSe such as GaAs, GaN, GaP, and InN as well as InP in III-V group semiconductors (Figure 1.9). In particular, GaAs and InP have direct band gap, also similar bulk band gap compare to CdSe. However, GaAs has the same limitations as CdSe because it contains Arsenic that is one of class B toxicity materials. While InP has neither Class A elements (Cd and Hg), nor Class B elements (As and Se). So increasing research effort of InP quantum dots has been published in recent years. The researches have reported many research results such as method of InP quantum dots as efficient emitters as covering blue to near infrared[21], large scale synthesis of InP quantum dots[22], Cu-doped InP quantum dots[23], and InP@ZnSeS gradient shell quantum dots[24]. Recently, InP quantum dots have been used flexible QD-LED[25] and color conversion devices[26].

The other cadmium free quantum dot is I-III-V semiconductor materials. CIS (Copper Indium sulfide) quantum dots have received considerable attentions due to interesting optical properties and low toxicity. These materials can be controlled optical properties by ratio control between copper and indium[27]. The unique properties of CIS QDs are broad emission wavelength and larger FWHM than CdSe quantum dots. So CIS QDs have been reported as efficient emitters in Color conversion device to make white light emitting diodes (WLED).

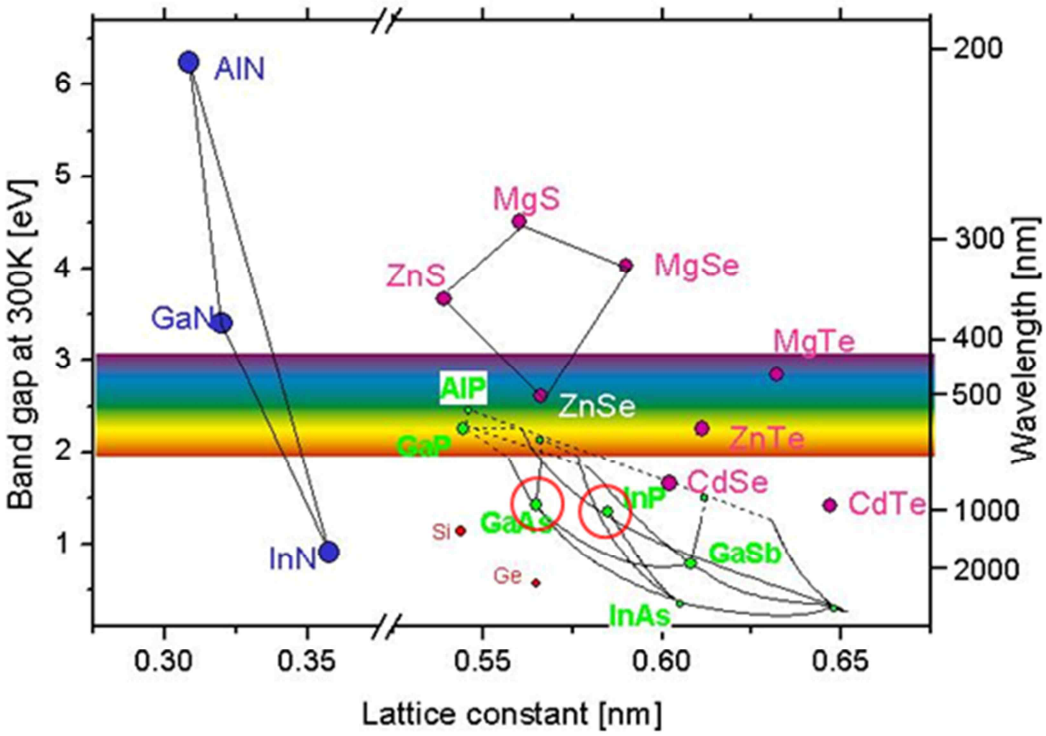

Figure 1.9 Various band gaps and lattice constant of II-VI, III-V group semiconductors (from http://www-opto.e-technik.uni-ulm.de/lehre/cs/)

Advantages	Disadvantages
1. Low toxicity of III-V quantum dots 2. Band gap tunable properties of III-V quantum dots 3. Less ionic lattice, larger exciton diameters of InP 4. Apply various organometallic precursors	1. Difficultly synthesize and control III-V quantum dots 2. Low crystallinity of III-V quantum dots 3. Poor optical properties and stabilities of III-V quantum dots

Table 1.2 Advantages and disadvantages of III-V quantum dots to alternate CdSe

1.3 Quantum dots color conversion devices

Illumination is one of the largest energy used fields that globally consumes about 20% of electronic energy[11]. The steadily increasing energy consumption has made the concerns of climate change and global warming phenomena, so the development of high efficiency light sources has been emphasized to reduce energy consumption. The quantum dots, that have excellent optical properties (high luminous efficiency, narrow full width at half maximum, band gap control by size, etc.), attracted considerable attention as a next generation materials in a variety of optical devices. Also, QDs are available to use solution process (spin coating, mist, coating, inkjet printing and micro-contact printing) in device fabrication. Among the various application areas with excellent optical properties of QDs, one of active research fields is QD color conversion devices. The applications both QD-LED and QD color conversion devices are called optical devices in common but the operating mechanism and the development direction between QD-LED and QD color conversion devices are different. First, a look at the QD-LED mechanism, the holes and electron are injected directly into the active layers then radiative recombination occurs in the active layers. While the mechanism of QD color conversion devices is a kind of energy transfer between QD layers and adjacent larger band gap materials so QDs reabsorb emission of adjacent larger band gap materials to generate QDs emission. Moreover, pursing development direction of QD-LED is facilitating more saturated blue, green, red color than commercial HDTVs for next generation LED. While the key point of QD color conversion device is high quality white light demonstration for next generation illumination. Table 1.3 shows the typical performance of commercial WLEDs and QD based WLEDs. The incandescent bulbs emit high quality white light (CRI = 100) but that consume about 80% by heat generations. The fluorescent lamps and HIDs are inexpensive and make strong white light, but quality of white light of them is poor. So we will need the next generation WLEDs that have the advantages of incandescent and fluorescent light at the same time, and the representative candidate is QD based WLEDs. Especially, comparing to QD-LED, QD color conversion devices have been studied from university labs to large companies such as Samsung[3], and QD-vision (Figure 1.10). This is evidence that QD based WLEDs have been getting even closer to commercialization. In this section, recent research trends of QD color conversion devices will be mentioned by dividing into discrete color mixing WLEDs, Cadmium based color conversion WLEDs, Cadmium free color conversion WLEDs.

Light source	Output [lm]	Wattage [W]	LE [lm/w]	CCT [K]	CRI	Cost [$*kl/m]	Lifetime [hr]
Commercial WLED	20 – 45	1	72 -101	3300 – 5500	70 – 90	5 – 20	50000
Incandescent Bulb	850	60	14	3300	100	0.4	1000
Fluorescent Lamp	5300	32	83	4100	78	1.5	20000
HID	24000	400	80	4000	65	1.0	24000
InP QD Based WLED[21]	N/A	N/A	10 – 20	3200 – 6500	86	N/A	N/A

Table 1.3 The typical performance of general light sources (commercial WLED, incandescent bulb, fluorescent lamp, high intensity discharge lamp) and InP QD based WLED[11]

Figure 1.10 Examples of QD-color conversion devices by large companies[3](from Sony electronics website-left)

1.3.1 Discrete color mixing WLEDs

The simplest main idea of fabricating white color was mixing three primary colors (red, green, blue emitters) appropriately until the early 2000s. The conventional phosphors such as $Y_3Al_4O_{12}:Ce^{3+}$ are widely used in conventional light sources, which generate yellowish white lights as limit of phosphors. So next generation WLEDs must need additional emitter to compensate phosphor's weak points. The core-shell structure CdSe QDs have be widely used to fabricate discrete color mixing due to simple core tuning methods (Ex: size, composition, etc.).There are only QD discrete mixing WLEDs and organic & inorganic hybrid type WLEDs in this application. The Bawendi group is one of the advanced groups in quantum dots. They published a considerable result about only QD discrete mixing WLEDS in 2007[28] (Figure 1.11 (a)). In this study, CdSe QD monolayer of suitable mixing ratio (red: green: blue = 1:2:10) is applied devices by simply spin coating. The red QDs need a relatively small amount in the QD mixture, because that has additional light emitting mechanism unlike blue QDs, which can reabsorb from emission of green, blue QDs and occur red emission. The similar phenomenon occurs between green QDs and blue QDs. But the optical properties of QDs monolayer were hard to maintain for a long period due to high temperature by LED operation. Several studies have suggested a solution to create hybrid QD layers by mixing organic materials (=charge transfer materials) and various color QDs[29] (Figure 1.11 (b)). The important point of hybrid layers is to fabricate monodisperse mixture mixing QDs and organic materials that can induce active energy transfer condition. Moreover, when simple spin coating is used for making large area QD monolayers, spin coating can induce phase separation and aggregation of QDs[30]. To solve this problem, the researchers have suggested PDMS micro-contact printing method to alter spin coating[31] (Figure 1.11 (C)). When micro-contact printing method is applied devices, the under organic layers of LED can avoid contact with non-polar solvent. This advantage can enhance device stabilities by minimization of defects. The key point of this method is to apply barriers such as SU8 between PDMS and QDs, because PDMS have solubility in nonpolar solvents such as hexane, chloroform.

Nevertheless, discrete color mixing WLEDs has several limitations which are as follows.

① It is difficult to find a condition that the optical properties of each QDs are maintained when we fabricate WLED.

② The overall PL QY of QDs must decrease by reabsorption among QDs.

③ We must need very uniform size QDs for a good discrete color mixing.

Because of these limitations, in recent years, research in this field has declining trends and color conversion WLEDS have received attentions as a special alternative.

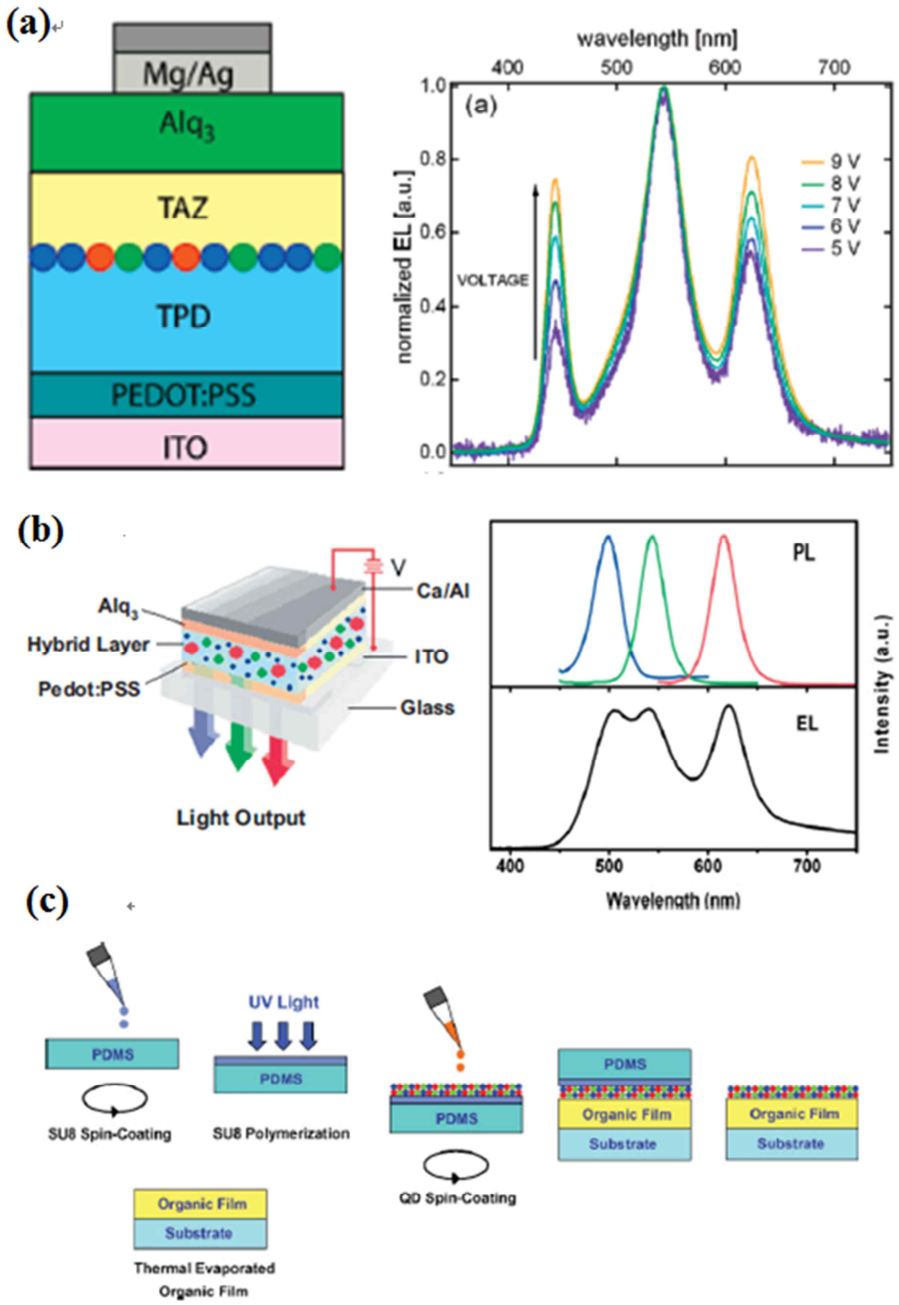

Figure 1.11 The example of discrete color mixing WLEDs (a) only QD discrete color mixing WLEDs[12] (b) organic/inorganic hybrid color mixing WLEDs[29] (c) fabrication step of QDs PDMS micro-contact printing method[31]

1.3.2 Cadmium based QDs color conversion WLEDs

The QD color conversion WLED began with the introduction of the QDs to break through the limitations of the color conversion devices using a variety of conventional phosphors. There are several weak points of conventional phosphors as follows.

① Difficult to control the composition of phosphor layers

② Not simple to adjust PL properties of phosphors (Difficult to tune color parameters)

③ Hard to make uniform films

④ poor thermal stability (PL QY is dramatically decreased at high temperature)

For an example, the typical performance of the phosphor color conversion WLEDs is represented at figure 1.12 and table 1.4[32]. These devices have 80~85 value of CRI (color rendering index) and low luminous efficiency. Also, PL peak shapes of phosphors were hard to be changed by concentration control of phosphors. The researchers in the U.S. department of Energy have recommended the several targets for WLEDs that were generally used in this field.

① CIE (commission Internatial de l'Eclairage) chromaticity coordinates: (0.33. 0.33) (= sunlight)

② CRI (Color Rendering Index): >80 (CRI of sunlight: 100)

③ CCT (Correlated Color temperature): warm white (2500 ~ 4500 K), Cold white (4500 ~ 6500 K)

④ Luminous efficiency: 200 lm/W

If you want to high quality WLEDs, you have to need additional emitter that has red emission. But, 3 types of phosphor are hard to use together in a WLEDs because of difficulty of optimization among three phosphors concentration. To solve this problem, the quantum dots have received large attentions as a color conversion material since early 2000s. The concepts of QD color conversion devices are divided into only QDs types and QDs + phosphors types that are similar to discrete color mixing WLEDs.

Especially, Cadmium based QD color conversion devices that consisted of various color QD conversion filters on the blue LED (GaN or InGaN LED) have been widely studied in a number of papers since 2000s.The general researches of only QD type Cd based QD color conversion devices are introduced through figure 1.13(a) among various researches of them[33]. In this paper, QD conversion filters were made by mixing QDs and PMMA. Also, QD conversion filters were made up in order of the blue LED/Green QDs/Red QDs to induce subsequent color conversion. Nowadays new generation color conversion devices must have long lifetime, low CCT (2500~4500 K) to provide comfortable light for people as well as strong intensity emission, because the purpose of new color conversion devices is to replace the commercial lamps. But the typical core-single shell structure QDs have a limitation that is degradation by high temperature (100 ℃) of LED chip. As solutions of them,

the researchers have attempted various changes of QDs and device fabrication steps. The efficient change of QDs was multi-shell QDs. The multi-shell CdSe QDs enhanced stability as soon as band gap control by thick shell, so lifetime of color converter was increased[3] (Figure 1.13(b)). The multi-shell was synthesized by additional hot injection of shell precursors and heating up with washed core-shell structure CdSe (green = CdSe@ZnS QDs, red = CdSe@CdS@ZnS QDs) and shell precursors. This paper proved that CdSe QD color conversion WLED can be used as LCD backlight and which can express wider colors than HDTV. Also, this paper was published by Samsung Advanced Institute of Technology that is evidence closer to commercialization of QD color conversion devices. Moreover QD-Vision and Sony Corporation has made a TV with a similar form, and 3M has developed a flexible on color filter called Quantum dot enhancement film (QDEF).

The general surface of CdSe QDs consists of fatty acid such as oleic acid. That has made some problems during production of QD color conversion filters. The matrix materials and the QDs weren't mixed uniformly and then QDs were aggregated on surface of the filters. Another alternative for stability enhancement of device is ligand exchange of QDs surface. For example, the researchers exchanged the ligand of CdSe QDs from Oleic acid to thiol containing organosilicate ligand then mixed with surface modified QDs and organosilicate materials for matrix[34] (Figure 1.13(c)). As a result, they can make homogeneous QD/OS hybrid filters due to similar functional groups between QDs and OS. Also, optical properties and chemical stabilities were enhanced by this ligand exchange steps unlike conventional ligand exchange methods.

The other method to enhance stability of QD color conversion devices is silica coating method. The typical silica coating method is reverse micro-emulsion method that was widely used for surface coating of nanoparticles such as metal, metal oxide, and QDs. However micro-emulsion method usually gives adverse effect for silica coated QDs such as PL intensity decrease. In order to solve the limitation of classic silica coating, the researchers published a silica coating method recently in a different way. The key point of this study was the silica sol-gel reaction using propylamine (as catalyst) and 3-mercaptopropyltrimethoxysilane (MPS) after a ligand exchange by using 6-mercaptohexanol (6-MHOH)[35]. They proved enhancement of thermal stability at high temperature and prevent of self-quenching and PL QY decrease for using this method.

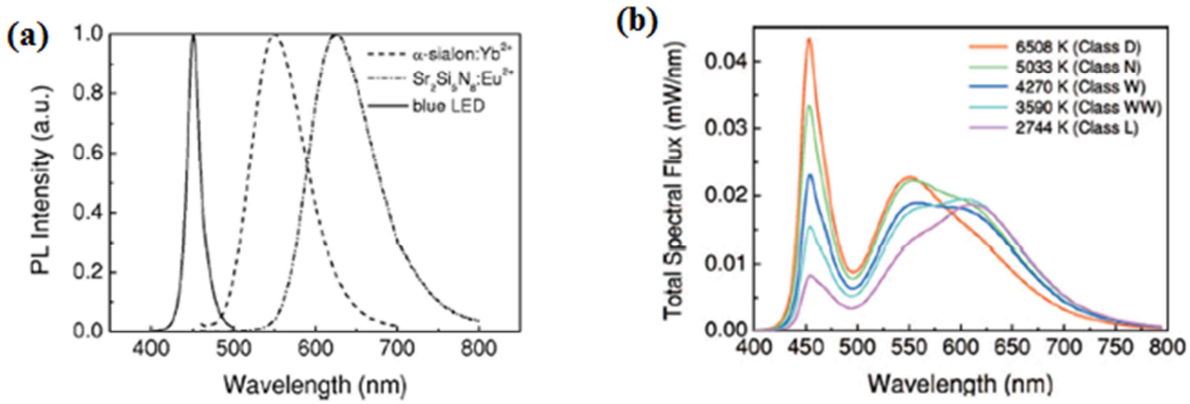

Figure 1.12 (a) PL emission spectrum of α-sialon: $Yb2^{+}$ and $Sr_2Si_5N_8:Eu^{2+}$ phosphors (b) EL emission spectrum of various type WLED using α-sialon: $Yb2^{+}$ and $Sr_2Si_5N_8:Eu^{2+}$ phosphors (class D =daylight, class N=neutral white, class W =white, class WW=warm white, and class L=incandescent light bulb)[32]

Class	L	WW	W	N	D
CCT (K)	2744	3590	4270	5033	6508
CIE *x*	0.461	0.402	0.372	0.344	0.313
CIE *y*	0.419	0.393	0.382	0.346	0.330
R_a	83	83	83	83	82
Luminous efficacy (lm/W)	17	20	21	22	23

Table 1.4 Optical properties of various types of 2 phosphors WLEDs class D =daylight, class N=neutral white, class W =white, class WW=warm white, and class L=incandescent light bulb)[32]

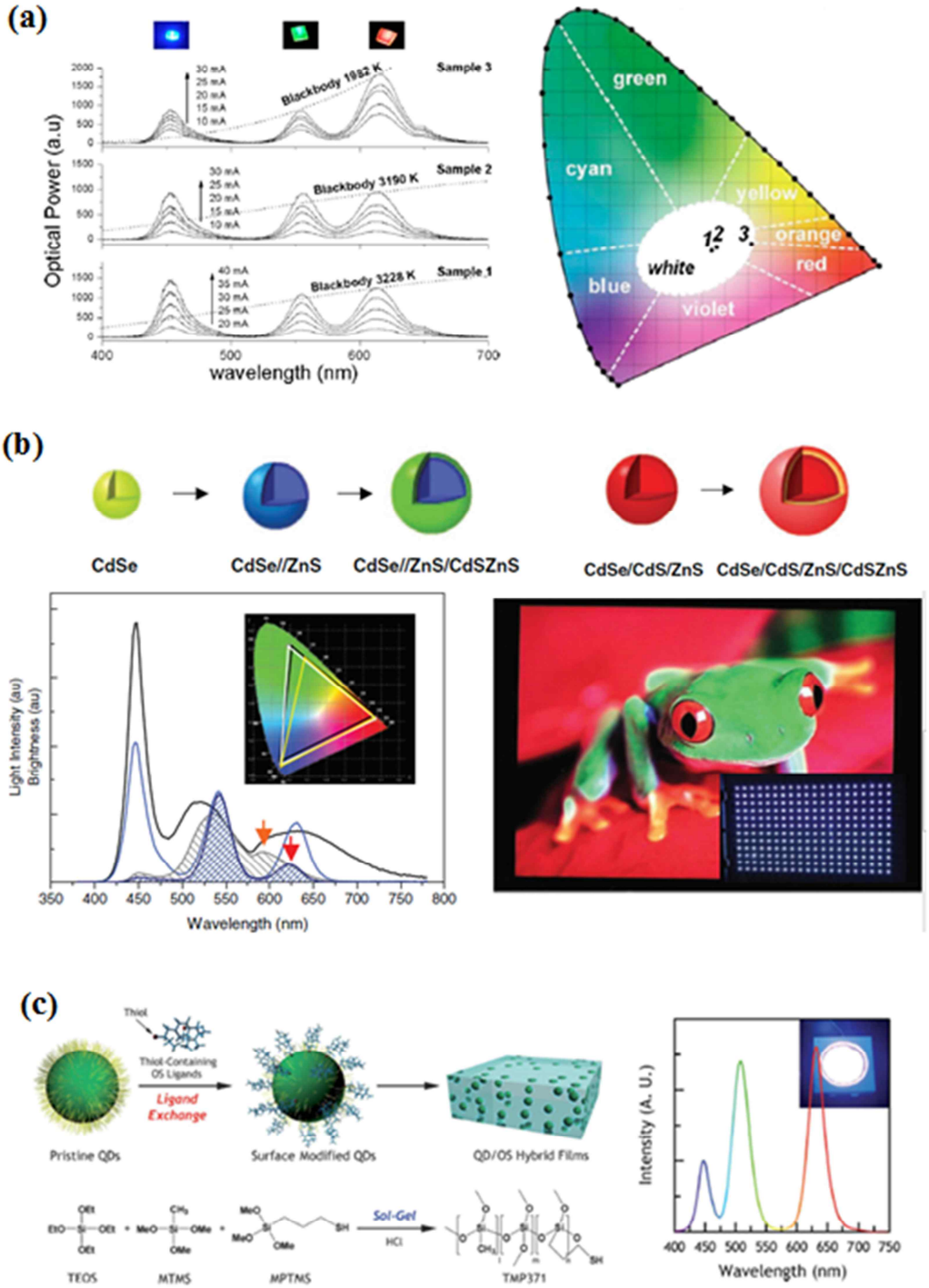

Figure 1.13 (a) an example of only CdSe QD based color conversion devices (red QDs concentration control)[32] (b) core-multi-shell CdSe QDs color conversion devices for display backlight[3] (c) an example of ligand exchanged CdSe QD based color conversion devices (thiol contained ligand exchange)[34]

1.3.3 Cadmium free QDs color conversion WLEDs

The Cadmium toxicity issue has been also remained in color conversion WLEDs. In order to solve this problem, the researches of cadmium free QDs color conversion WLEDs have been actively published since early 2000s. Unlike QD-LED, broad strong emission of QDs can be efficiently applied in this field to make high quality white light. So I-III-VI QDs such as CuInS2 QDs (CIS QDs) have been actively studied to alter phosphors. Especially CIS QDs have very broad (FWHM = 100~150 nm) and high intensity emission (PL QY >60%), moreover CIS QDs can be controlled colors from green to deep red by composition control (Cu/In)[36], Zn passivation[37], reaction time[38], etc.. The synthesis methods of CIS QDs were more flexible than synthesis methods of CdSe QDs then many new methods of CIS QDs have been reported recently. In this introduction, I will introduce some representative results among various studies of them. The WLEDs fabricated with Cu/In = 1/4 based CIS@ZnS QDs and blue LED showed potential to use blue-to yellow color conversion devices, just like widely used YAG : Ce phosphors[36] (Figure 1.14(a)). In other recently paper, Silica coated CIS QDs by solvothermal method enhanced thermal stability in YAG : Ce phosphors and silica coated CIS QDs mixed WLED[39].

The III-V InP QDs were hard to apply color conversion devices owing to poor thermal stability and low color conversion efficiency. Nevertheless, the researchers studied about InP QDs color conversion WLEDS in several concepts to overcome limitation of InP QDs. Of course, the simple type (=InP QDs + resin mixed type) of InP color conversion devices were published recently[26]. But simple types is hard to use making WLEDs by mixing with other emitters. So we needed special concepts for InP QDs color conversion WLEDs. One of them is WLEDs made by Green phosphor ($Sr_{0.94}Al_2O_4:Eu_{0.06}$), Yellow phosphor (YAG: Ce), silica coated red InP QDs[40] (Figure 1.14(b)). In this study, the researchers applied micro-emulsion method for silica coated InP QDs, but they mentioned week points of methods such as little agglomeration and luminescence decrease. Moreover, micro-emulsion method of QDs was famous for hard optimization then reaction conditions of methods vary by many papers and materials.

The ultimate goal of those who study this field is mass fabrication of nontoxic, flexible, and high performance WLEDs without CdSe QDs. For this goal, we will need a lot of studies to deal with Cadmium free QDs for color conversion materials.

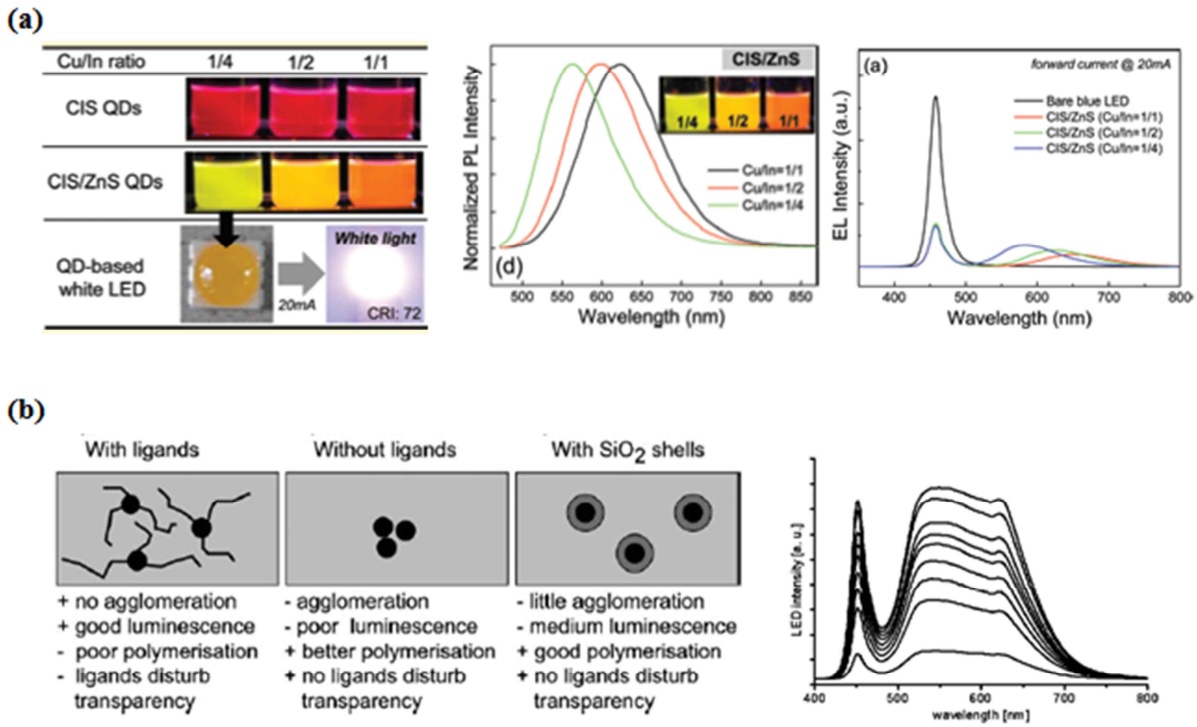

Figure 1.14 (a) the example of CIS QDs color conversion WLEDs by control Cu/In ratio[36] (b) silica coated InP QDs/Phosphors hybrid color conversion WLED by micro-emulsion method[40]

CHAPTER 2

A facile method to synthesize group III-V, Gallium phosphide Quantum Dots with controlled band gaps and their Application as Color Converters of LEDs

2.1 Introduction

The semiconductor nanocrystals, especially II-VI group semiconductors, have attracted noticeable interest because they exhibited excellent optical (tunable, narrow, and symmetric emission) and chemical properties different from those of bulk materials and phosphors. For this reason, II-VI group semiconductor nanoparticles, called II-VI group quantum dots (QDs), have found many applications such as light emitting diode (LED) [9, 12], bio application[14], and photovoltaic devices[41, 42]. Despite a lot of advantages of II-VI group QDs, the intrinsic toxicity of cadmium (Cd) and lead (Pb) has restricted their applications for commercialization. To overcome the limitation of them, III-V group QDs have been regarded as one of the potential alternatives, but the researches were just focused on indium phosphide (InP) QDs as core-shell structure[21, 24], alloyed QDs[22, 43], and metal doped QDs[23]. By developed InP QDs, the wide ranges of application have applied InP QDs with non-toxic concept since the late 2000s, but the lack of materials having the similar quality comparing to InP QDs has emerged.

The bulk Gallium phosphide (GaP) is indirect semiconductor with a band gap of 2.22 eV (559 nm) and many important uses in the microelectronics devices. Since 1990s, some papers have been published about the synthesis and characterization of GaP nanomaterials. The one of first synthesized nanocrystalline GaP were obtained by dehalosylation reaction in 1994[44]. Through the further studies in 1990s, nanocrystalline GaP were obtained by decomposing organometallic precursors[45, 46], and a single precursor[47]. However, the developed nanocrystalline GaP had some breaking points. First, the very long reaction time of at least 10 hours was required to synthesize nonocrystalline GaP. Second, the products have a fairly broad size distribution and shape of the products was not totally controlled. From these reason, we just confirmed nano-size gallium phosphide by XRD and TEM analysis in 1990s. Since the 2000s, the methods for synthesis of nanomaterials were rapidly developed and diversified. So, many researchers have attempted applying various developed methods to synthesize skillful GaP nanocrystals. Representatively, Kim et al. suggested a synthetic route by thermal

decomposition of $Ga(P^tbu_2)_3$ in surfactant to obtain GaP nanoparticles and nanorods[48]. Gao et al. applied solvothermal method[49] and presented aqueous synthesis[50] of GaP nanocrystals. Recently, GaP nanoparticles were synthesized by using ion exchange method[51] and transmetalation route[52]. However most of previous studies about GaP nanocrystals can't perfectly solve the problems about the GaP nanoparticles such as the poor optical properties and low crystallinity to apply optical devices (ex: QD LEDs and color conversion devices). Moreover, in ion exchange method, some Cadmium atoms were remained (Ga: Cd= 8.8: 1) in GaP nanocrystals in $Ga3^+$ exchange reaction of Cd_3P_2 nanoparticles[51]. To solve problems of previous studies, we approach synthesis of GaP nanocrystals by batch method because this method was widely used to obtain various colloidal nanomaterials. Especially, InP QDs can be synthesized using TMS_3P in short reaction time. On the other hand, GaP QDs were hard to be synthesized due to the absence of gallium precursors to make suitable precursor combinations with TMS_3P. In this study, we proposed a suitable gallium precursor to make colloidal GaP QDs by batch method. Also, we presented a facile hot injection method for colloidal GaP QDs and investigated improved optical properties of GaP QDs in comparison with previous studies. Furthermore, the GaP QDs color conversion devices were fabricated on the blue LED and UV-LED, and showed the possibilities as next generation color conversion materials for WLEDs.

2.2 Experimental

2.2.1 Materials

Gallium (III) acetylacetonate ($Ga(acac)_3$, 99.99% trace metal basis), gallium(III) chloride (anhydrous, ≥99.999%), oleic acid (OA, technical grade), 1-octadecene (90% technical grade), 9,10-diphenylanthracene and trioctylphosphine (TOP, 97%), lauric acid (≥98%), palmitic acid (≥99%), stearic acid (95%, reagent grade), myristic acid (≥99%, sigma grade) were purchased from Sigma-Aldrich. Tris(trimethylsilyl)Phosphine (TMSP, 95%) was ordered from JSI silicone Co. Ltd. Gallium (III) acetate (99%) was purchased from ALFA chemistry. Hexane, ethanol, acetone were from Samchun pure chemical. n-Butanol (HPLC, 99.7%) was purchased from Daejung chemicals & metals Co. Ltd. Coumarin 510 was ordered from Exciton.The Secure 8110 ultraviolet curing adhesives were purchased from Fotopolymer. All chemicals were used without further purification. UV-LED chips (model CUN6AF1A) were purchased from SEOUL VIOSYS.

2.2.2 Preparation of colloidal Gallium phosphide quantum dots

The schlenk line techniques were used at all experiments. A typical synthesis of gallium phosphide quantum dots with a PL Peak ~520 nm (=green emission) was as follows. Gallium acetylacetonate (0.366 g, 1 mmol), oleic acid (0.45 ~ 0.55 mmol), and 1-octadecene (4 ~ 5 ml) were loaded in three-neck flask. The mixture was degassed under vacuum for 30 min at room temperature, followed by purging with argon gas during an hour. Then, the solution was heated to 300 ℃ (9 ℃/min) and rapidly injected about 1 ml mixing solution (2 mmol TOP + 0.5 mmol $(TMS)_3P$). The temperature of solution was dropped about 285 ℃ due to hot injection. The solution was rapidly heated to 300 ℃ and maintained for 30 min under argon atmosphere. The result colloidal solution was cooled to room temperature under argon gas flow and precipitated by using ethanol, acetone, and butanol mixing solution. Product was perfectly precipitated by centrifugation at 7000 rpm for 5 min and supernatant was decanted. The washing step was repeated 3 ~ 4 times, and product was dispersed in hexane. The gallium phosphide QDs with various band gaps can be prepared by control of precursor ratio.

2.2.3 Characterizations of gallium phosphide quantum dots

UV-vis and PL spectra were recorded on a Shimadzu UV-2450 spectrophotometer and Cary Eclipse (Varian) fluorescence spectrophotometer, respectively. Powder X-ray diffraction was obtained using a Rigaku MAZX 2500V high power x-ray diffractometer. All transmission electron microscopy (TEM) images were taken on JEOL JEM-2100 transmission electron microscopy operating at an acceleration

voltage of 200 KV. The room temperature quantum yields (QY) were measured by comparing to reference dyes both coumarin 510 (Green dye) and 9, 10 diphenylanthracene (blue dye).

2.2.4 Fabrication of InGaN/GaN blue LED chips

In order to grown LED structures having a InGaN/GaN MQW structure, 50 nm-thick GaN buffer layer, a 2.5 um thick Si-doped n-type GaN layer, a 5-period InGaN/GaN MQW structure, and a 200 nm-thick p-type GaN layer were epitaxially grown on 2 inch sized (0001) Patterned sapphire substrate by using metal-organic chemical vapor deposition(MOCVD). To fabricate LED chips, the mesa structure was formed by using an inductively coupled plasma system, to expose the *n*-GaN layer for *n*-type ohmic contact formation. ITO based *p*-electrode was deposited onto the InGaN top layer both as a current spreading and light transmitting layer. Then, Cr and Au were deposited onto both the exposed *n*-type GaN layer and the ITO layer for *n*- and *p*-type electrodes, respectively. After the sapphire substrates were lapped, they were diced into individual chips with a size of 1,200×650 um^2. Note that we also scribed the substrate after the lapping of the sapphire substrate using diamond tip. Finally, LED chip was attached on LED package (9080type). The electrical and optical properties of both LED samples were measured by using the optical spectrum analyzer and the precision semiconductor parameter analyzer, HP 4145B. The light output power and far-field radiation patterns were measured on non-encapsulated LEDs in chip form.

2.2.5 Fabrication of Remote type GaP QDs color conversion LEDs

The synthesized GaP QDs in 50 μℓ hexane mixed with Secure 8110 ultraviolet curing resins (UV resins) by vortexing. The homogenous mixtures of GaP QDs and UV-resins were poured in a circular mold then mixtures were cured by UV light of 365 nm emission during 5 minutes. The solidified color conversion film was picked off from molds. Those films were put on LED chips to fabricate remote type color conversion LEDs.

2.2.6 Characterizations of Remote type GaP QDs color conversion LEDs

To record EL spectrum, we fabricated customized a zig system like figure 2.1 and the overall measurement system containing the fiber optical cable were used from Led chips tester ELT-1000 (Ecopia Corporation). In characterization steps of color converters, the LED chips were completely fixed on the plate to prevent chips moving during measurement. Also, the position of the optical cable

was fixed to optimize the maximum intensity of the bare blue LED emission. Following optimization of LED chip and optical cable positons, EL spectrum of color conversion LEDs were recorded while replacing the GaP QDs color converter film. The key point was to put color converter film in parallel on LED chip. Also, all measurement was conducted on same blue, UV LED chip. Color conversion efficiency of device was calculated by integration of EL spectrum.

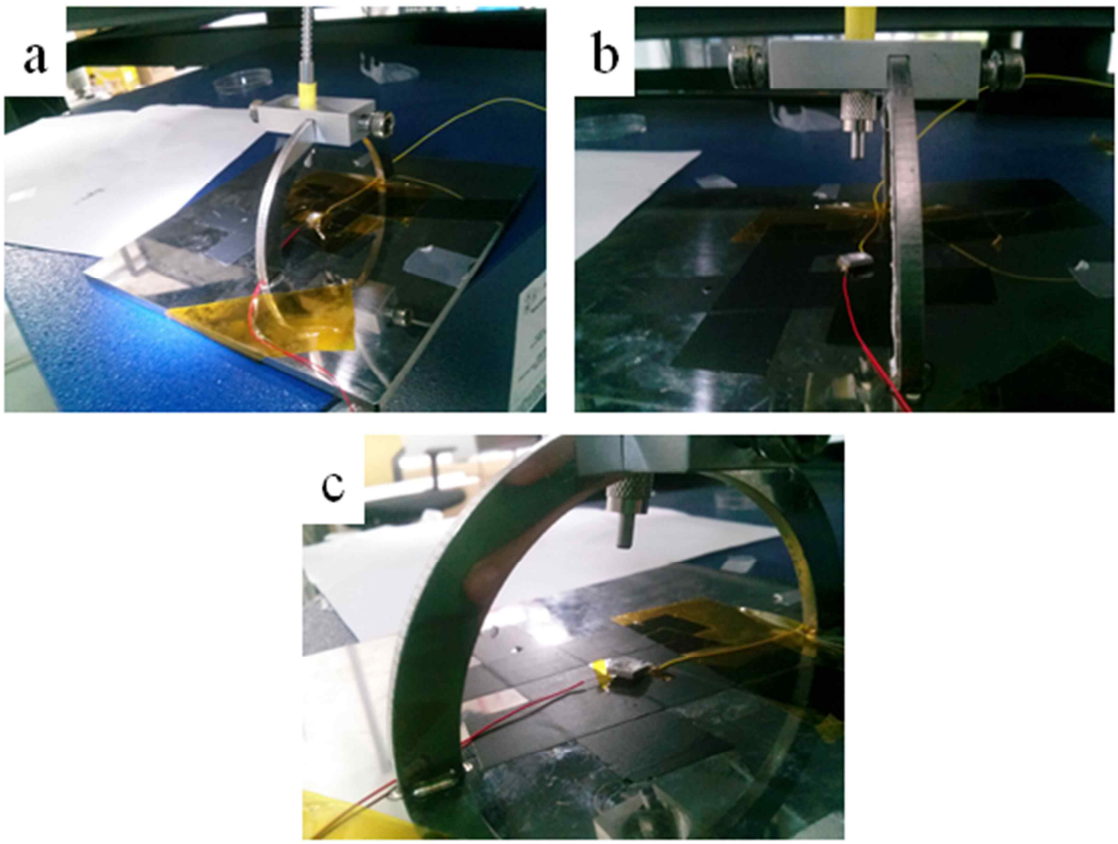

Figure 2.1 (a) The customized jig system to measure GaP QDs color conversion devices, (b)-(c) Zoom in images of zig system

2.3 Result and Discussion

2.3.1 The synthetic mechanism of GaP QDs

The GaP colloidal quantum dots were synthesized using gallium acetylacetonate ($Ga(acac)_3$), tris(trimethylsilyl)phosphine ($(TMS_3)P$), 1-octadecene (ODE), oleic acid (OA), and trioctylphosphine (TOP). ODE is one of typical noncoordinating solvents, which is widely used to synthesize colloidal nanomaterials such as metal oxide and quantum dots. Also, OA and TOP are typical surfactants for synthesis of nanomaterials. Figure 2.2 illustrated the overall synthetic procedure. In the brief procedure, the gallium oleate complex was obtained by slowly heating up a mixture of gallium acetylacetonate and oleic acid in ODE solvent under inert condition. In this step, the chemical bands between gallium and acetylacetone were exchanged for the chemical bands between gallium and oleic acid by heating up. As a evidence of the reaction, the opaque solution mixed with ($Ga(acac)_3$), ODE, and OA was gradually changed into the clear yellowish solution by heating up to high temperature (300 ℃). This phenomenon of gallium oleate was published in previous studies about synthesis of metal oxide[5] and quantum dots[53]. Moreover acetylacetonate ions made by gallium oleate preparation were easily removed by evaporation through bubblers owing to the low boiling point (140 ℃) of acetylacetonatone. We also conducted similar experiments using gallium acetate and gallium chloride to synthesize gallium oleate complex. However, gallium oleate complex were not synthesized by these experiments and the precursor mixed solution was maintained during heating up. The detailed procedures were described in experimental section.

2.3.2 XRD analysis for gallium phosphide quantum dots

The XRD patterns for the gallium phosphide were collected on Rigaku MAZX 2500V high power x-ray diffractometer using Cu-Kα radiation (λ = 1.5405 Å) operated for 2θ = 20 - 80° and with a scan rate = 2°/min. Figure 2.3 shows the high power X-ray diffraction (XRD) patterns that are matched to (111), (220), and (311) planes (2Θ=28.341, 47.128, and 55.910 respectively) of the zinc blende structure of the bulk GaP (JCPDS 72-4660) and the XRD patterns of GaP nanoparticles in previous studies[44, 46, 50]. The XRD patterns of bulk GaP semiconductor shows more multiple peaks than that of published GaP nanoparticles. Especially, this tendency was greatly intensified at the XRD patterns of synthesized GaP quantum dots in this study. So the reason of broadening in the peaks of XRD patterns can't be called just very small size of nanoparticles. Thus another reason of them can be implied to low crystallinity of GaP quantum dots. In order to check this assumption directly, we additionally analyzed particle size, and crystallinity of GaP QDs using TEM microscopy.

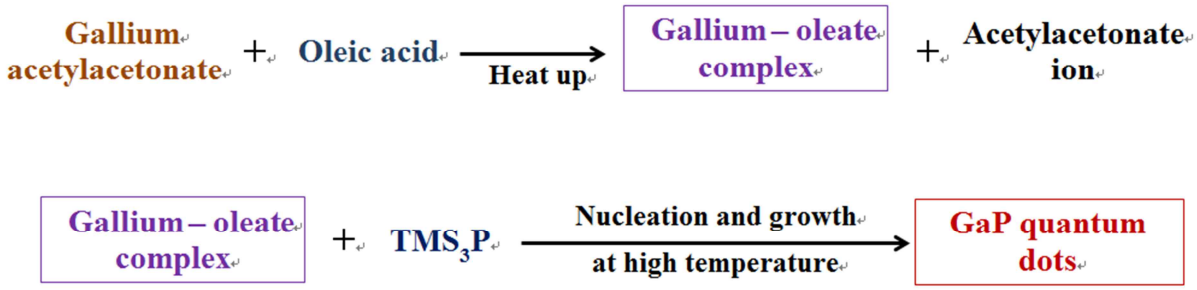

Figure 2.2 The Overall scheme of synthesis of GaP quantum dot

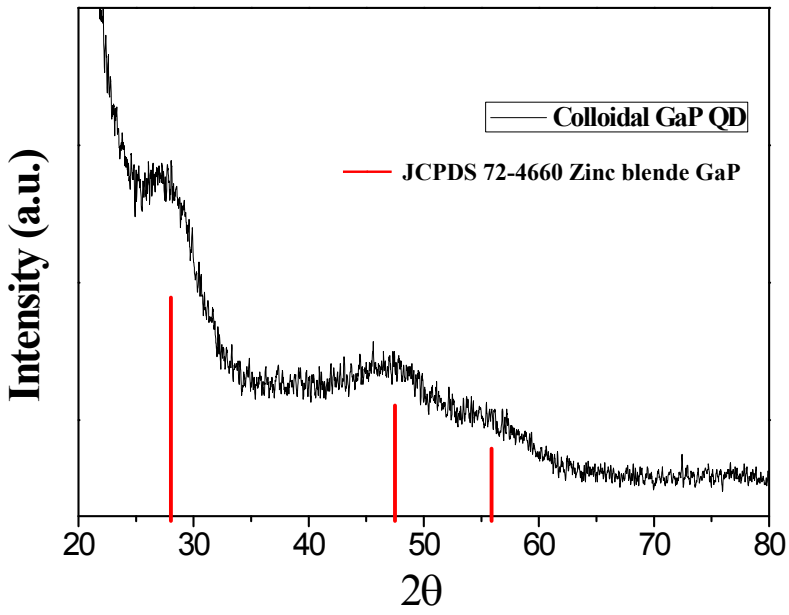

2 theta	Intensity
28.341	999
32.841	120
47.128	516
55.910	323
58.632	25
68.855	63
76.063	99

Figure 2.3 High power-XRD data of colloidal GaP quantum dots

2.3.3 Optical properties & TEM images of GaP QDs

Figure 2.4(c) shows various photoluminescence (left-520, middle-460, right-400 nm) of the GaP QDs dilute solutions on the 365 nm emission UV-lamp (LF-206-LS, Uvitec Cambridge).The GaP colloidal QDs were synthesized at various synthesis condition. Especially, surfactant amount control with fixing other synthesis condition was the best effective variable to control optical properties of GaP QDs in this method. Figure 2.4(a), (b) show changes of GaP QDs optical properties owing to OA amount control. These three conditions were optimized through numerous trial and errors to make typical synthesis conditions for each emission color. The first excitonic peaks in the absorbance graphs (Figure 2.4(a)) appeared at about 370, 440, 500 nm in case of the optimized GaP QDs with OA amount 2.4, 1.2, 0.55 mmol, respectively. These absorbance peaks showed a red shift as amount of OA decreased. Figure 2.4(b) shows the normalized photoluminescence peaks of the optimized GaP QDs at each OA amount condition. These photoluminescence peaks have PL intensity maximum wavelength 400, 460, and 520 nm, respectively. Also, a full width at half maximum (FWHM) of emission were approximately 60, 50, 75 nm in case of OA amount 2.4, 1.2, 0.55 mmol, respectively. The photoluminescence quantum deficiency (PL QY) were obtained by comparison with Coumarin510 (95% in ethanol), and 9, 10 diphenylanthracene (97% in cyclohexane). PL QY of the GaP QDs were calculated to 35~40% (OA 0.55 mmol, green), 15~20% (OA 1.2, 2.4 mmol, blue). Especially, PL QY (35~40%) of OA 0.55 mmol condition is an considerable high value as compared with PL QY of other only core form QDs such as CdSe, InP QDs, So that have the possibility to apply optical devices like LED and color conversion device. Figure 2.4(d) shows the transmission electron microscopy (TEM) image of the green emission (520 nm) GaP QDs. The green emission GaP QDs has a size of 2~3 nm. In the TEM image, we can check that GaP QDs have a low crystallinity once again and the difference of particle size between different surfactant conditions was hard to determine it.

In general, the researchers have reported continuous band gap control of the well-known colloidal QDs such as CdSe[54], InP[21] QDs in the direction of larger band gap compare to band gap of bulk materials due to quantum confinement effect. In contrast, Red shift trend of GaP QDs is different compared to other QDs. The other QDs such as CdSe and InP have continuous red shift by various synthesis condition, but GaP QDs fixed PL wavelength in three position and change ratio of each peak's intensity. For instance, photoluminescence peak of GaP QDs with OA 0.55 mmol condition was made with mixing 520 nm main emission, 460 nm secondary emission, and 400 nm feeble emission. In hot injection method, the Photoluminescence wavelength and particle size is gradually increased by reducing surfactant amount. The developed GaP QDs also follow this trend, however the particle size change is hard to observe because particle size of green emission GaP QDs is just 2 ~ 3

nm. Figure 2.5 shows the shape change of GaP QDs photoluminescence by adjustment of oleic acid amount from 1.2 mmol to 2.4 mmol. The OA 2.4 mmol condition of GaP QDs has a 400 nm single peak with a long tail, but a tendency, which is successively increase of the 460 nm peak intensity, was observed by decrease of OA amount in GaP QDs synthesis. The table in figure 2.5 shows intensity ratio between 400 nm and 460 nm emission in each of the synthesis conditions. The similar trend of peak shift can be observed between 460 nm and 520 nm emission. Figure 2.6 shows that synthetic progress is very unstable due to lack of surfactant. In OA 0.3~0.5 mmol condition, the synthesized gallium oleate was not changed for clear solution and remained some precipitates. Then crude solution in these conditions is showed in an upper inset image of figure 2.6 that is the unclear solution. If GaP QDs solution is obtained through the washing steps in these conditions, the product is also the unclear solution. Moreover aggregation easily happened in GaP QDs solution over a short period of time due to lack of surfactant. The less surfactant amount is used, the more these phenomena are intensified and the results of them can be confirmed in figure 2.6 (a), (b). The first excitonic peaks became increasingly unclear and the long tails were made in long wavelength because of opacity of solution (figure 2.6(a)). Photoluminescence peaks go against original trend (=figure 2.4, 2.5) and make the dual peaks (460, 520 nm peak) by blue shift. Of course, PL QY decreases sharply owing to lack of surfactant.

We conducted GaP QDs synthesis using various fatty acids ((lauric acid, palmitic acid, stearic acid, myristic acid). Figure 2.7 shows absorbance and photoluminescence of them. However the results were not impressive compare to oleic acid, and shape of absorbance and photoluminescence peaks were very similar to oleic acid. Moreover PL QY of them was calculated to 35~40% that was the similar result in comparison with oleic acid. Reaction time has been known as one of the important parameters in QDs synthesis (ex: CIS QDs[37], InP QDs[21], etc.).

In general, QD particle size is gradually increased and PL peaks are also red shift during increasing of reaction time. While the GaP QDs show similar optical properties (absorbance, Photoluminescence) in reaction time from 0 to 60 minute. Especially, three hours or more reaction time induced gelation of crude solution and poor optical properties. In typical GaP QDs synthesis, some by-products and remained precursors were contained in GaP QDs crude solution, which were separated from crude solution by washing steps. The reason of gelation was that unintended reactions among by-products, remained precursors, and GaP QDs occur during long reaction time. Also, we can't separate by-products and remained precursors in crude solution owing to strong bong strength.

We also tested various precursor ratios between $Ga(acac)_3$ and TMS_3P because synthesized gallium oleate and TMS_3P have different reactivity. When compared to the absorbance peaks, the overall peak shapes and position of the first excitonic peaks were very similar in various conditions (figure 2.8(a)). However, photoluminescence peaks show big differences by the precursor ratios. In Ga to P precursor

ratios 1/1 and 2/1, the overall peak shapes were maintained but PL QYs of them were different (2/1>1/1). Above 4 equivalents, the reaction not occurred properly due to lack of phosphine precursor and showed blue shifted peaks. Also, excessive amount of phosphine precursor induced negative effects in many sections such as optical properties, stability of QDs (figure 2.8(b)).

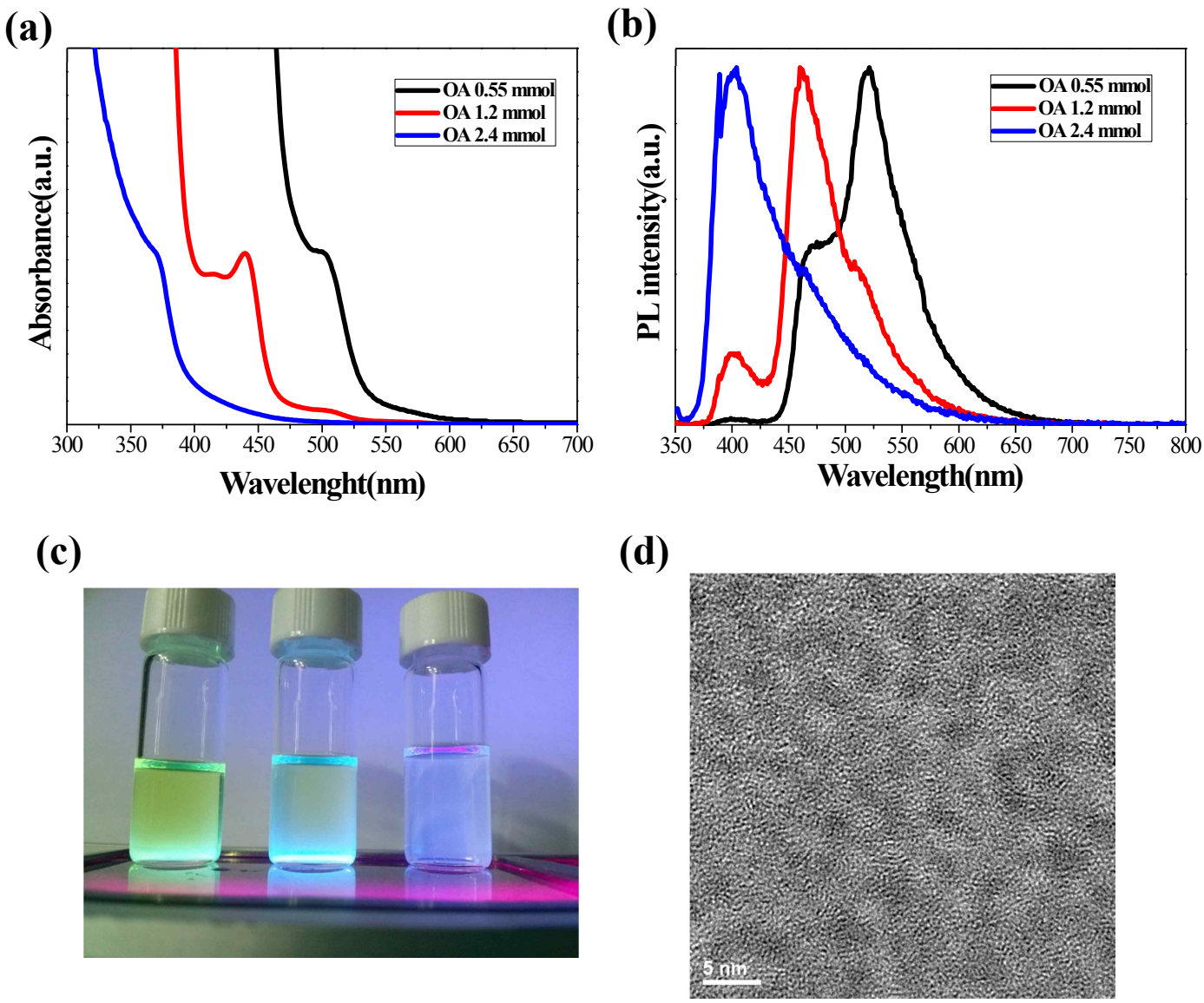

Figure 2.4 Normalized (a) absorbance and (b) photoluminescence spectra of surfactant amount controlled GaP QDs (OA 0.55, 1.2, 2.4 mmol) (c) photoluminescence of 520, 460, 400 nm emission GaP QDs solution (d) typical TEM images of green emission GaP QDs

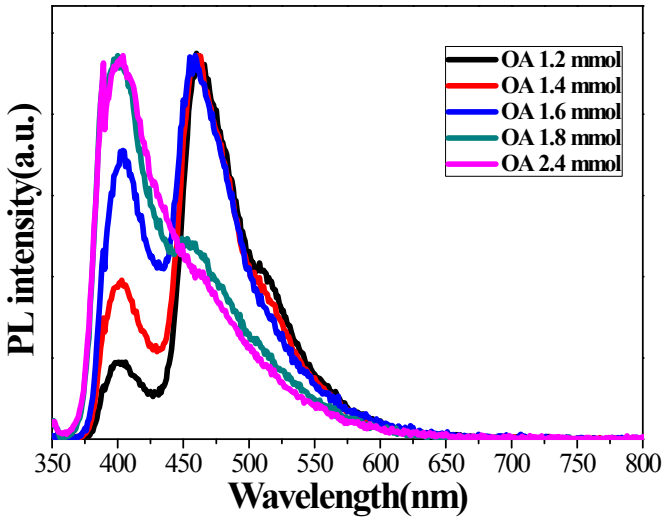

	454 nm peak : 400 nm peak
OA 1.2 mmol	**4.99 : 1**
OA 1.4 mmol	**2.41 : 1**
OA 1.6 mmol	**1.33 : 1**
OA 1.8 mmol	**1 : 1.91**

Figure 2.5 the shape change of GaP QDs photoluminescence by adjustment of oleic acid amount from 1.2 mmol to 2.4 mmol (PL Peaks were normalized at main peak of each graph)

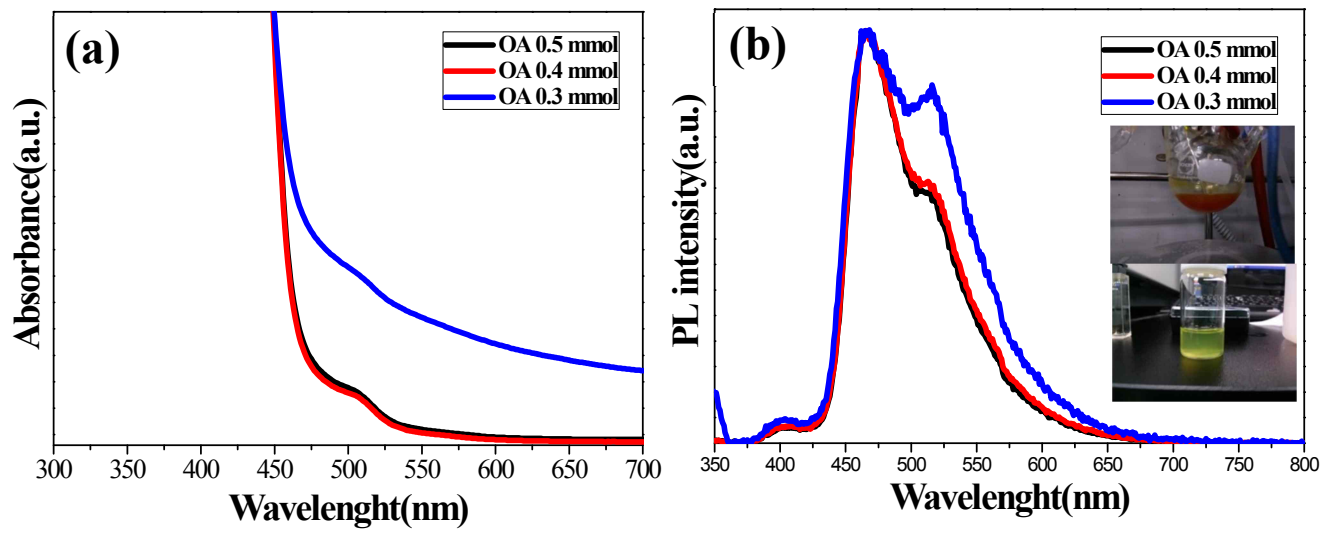

Figure 2.6 the optical properties change ((a) absorbance (b) photoluminescence by lack of surfactant, upper inset image-crude solution and bottom inset image-GaP QDs solution in OA 0.3 mmol condition

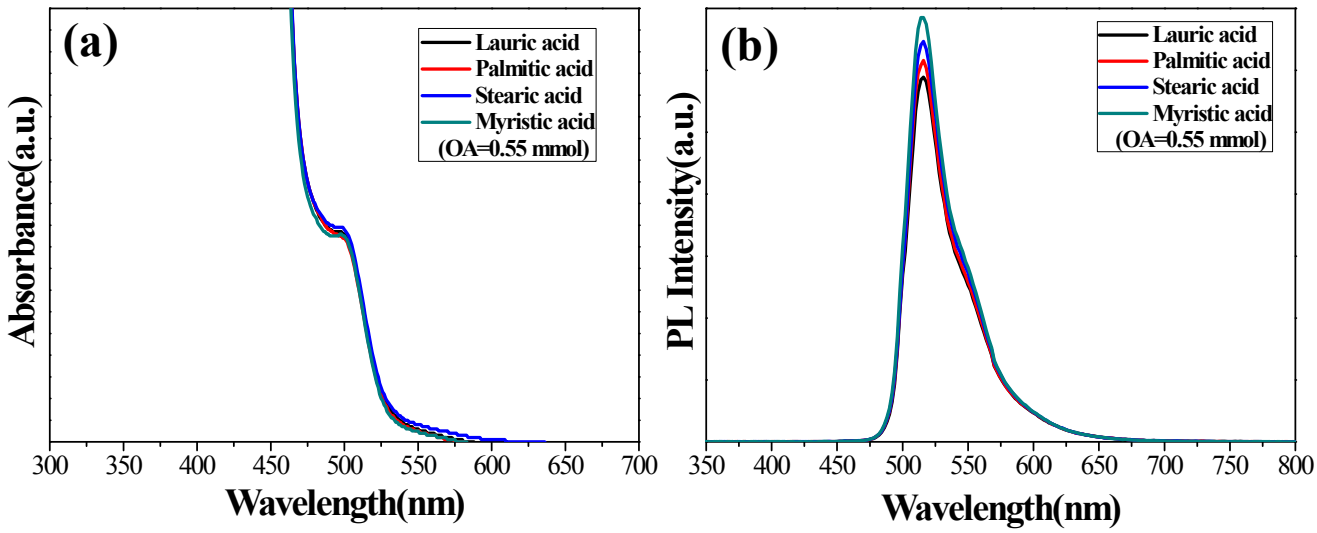

Figure 2.7 (a) absorbance and (b) photoluminescence(excitation wavelength: 500 nm) of GaP QDs using various fatty acids (lauric acid, palmitic acid, stearic acid, myristic acid) at same concentration of QD solution

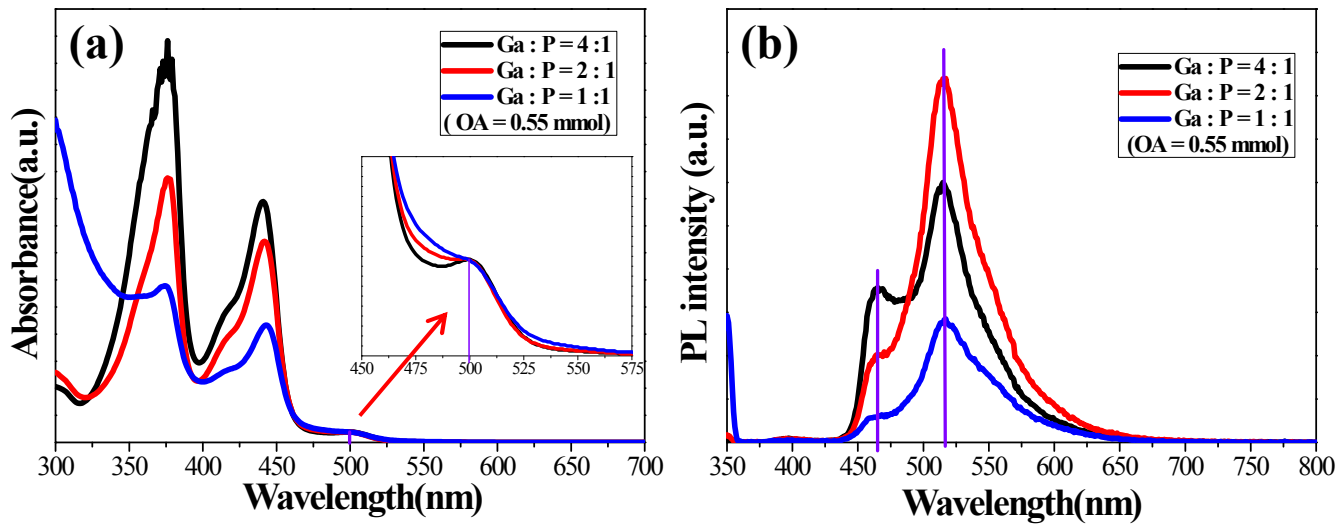

Figure 2.8 optical properties changes ((a) absorbance and (b) photoluminescence) of GaP QDs by various precursor ratios (Ga: P = 4:1, 2:1, 1:1) in same concentration GaP QD solution

2.3.4 Remote type GaP QDs color conversion devices

When cadmium based II-VI or III-V group (ex: InP, etc.) QDs are applied as color converters for WLED fabrication, PL QY of QDs is usually 50% or more. Therefore, developed GaP QDs in this study were hard to apply directly WLED fabrication due to lower PL QY than cadmium based II-VI or III-V group (ex: InP, etc.) QDs. However, green emission (520 nm) GaP QDs have a possibility to apply the color conversion devices because that have PL QY of about 35~ 40% and the device fabrication tests were intensively conducted to confirm a possibility of the green emission GaP QDs. In general Color conversion devices fabrication, UV-LED and blue LED were employed as the primary emission source and we also used them. EL spectrums of the remote type color conversion device fabricated with 1wt% GaP QDs blend on UV-LED were shown in Figure 2.9(a). The EL emission shapes by GaP QDs were very similar to photoluminescence shapes of green emitting GaP QDs in optimized QDs concentration (1wt%). In figure 2.9(b), the gradual increase of EL intensity was shown from 20 mA to 160 mA. The gradual tiny red shift of QDs color conversion peaks is also consistent with the result of previous QDs color conversion WLED[55]. We can see green emission that was made by operation of optimized GaP QDs color conversion device with UV-LED in figure 2.9(c). The color conversion efficiencies (CCE) of various QDs concentration converters with UV-LED were calculated by reduced UV-LED emission to GaP QDs emission ratio. The lower QDs concentration in blend mixed GaP QDs and UV resin induced the higher CCE of devices. Especially, in 0.5wt% concentration, CCE of device was about 40% that was similar value in comparison with solution PL QY of GaP QDs. However, in case of 0.5wt%, reduced UV-LED emission and formed GaP QD emission intensity was very small, so there was no significant meaning as color converter. On the other hand, more than 1wt% QDs concentration made clear green emission and we can clearly see green emission with the naked eye. Among more than 1wt% QDs concentrations, the highest CCE value was about 13% in 1wt% QDs concentration. Also, when QD+UV resin blend is made at 3wt% or higher QDs concentration, color conversion film can't be fabricated in a homogenous form and some cracks are created during UV curing steps due to QDs aggregation. Figure 2.10 shows the performance of the application when the blue GaP QDs used in the color conversion devices on UV-LED. The color conversion efficiencies of device with blue GaP QDs were lower than that of color conversion device with green GaP QDs, and the maximum CCE was 4.5% at 1wt% GaP QD concentration (figure2.10 (b)).

In general, QDs color conversion devices have received attentions as the next generation WLEDs. For this reason, GaN/InGaN blue LED were more widely used as the primary light source of QDs color conversion devices to fabricate WLEDs. To confirm the possibility of GaP QDs as materials for the next generation color conversion WLEDS, we also measured color conversion of GaP QDs about

the blue LED chips. Figure 2.11 shows performance of color conversion devices with blue LED. In these devices, we only used green GaP QDs because large parts of emission peaks overlapped between the blue GaP QDs and blue LED. The optimized EL spectrum was shown in figure 2.11(a) by fabricating devices at various QDs concentration. In this figure, the color conversion EL peak made by GaP QDs has a very similar shape in comparison with solution PL of green GaP QDs. Also, Figure 2.11(b) shows color conversion efficiencies at various QDs concentrations. The lowest concentration condition shows the highest CCE value (about 22%), but that has no significant meaning as color conversion devices due to the same reason like as UV-LED case (figure 2.12(a)). The CCE at the optimized condition was about 12% and CCE was gradually decreased by increase of QDs concentration. Owing to high Luminous efficiency of blue LED chip, we can directly detect detailed red shift of EL spectrum made by GaP QDs (figure 2.12(f)). At low concentration (0.5wt %), long tail was formed at long wavelength (>520 nm) then EL spectrum intensity was increased and formed a clear peak up to 2wt%. At more than 2wt% QDs concentrations, red shift and intensity decrease of peak were observed similar to upper color conversion device applied UV-LED (figure2.9). Through upper color conversion device results, we confirmed that color conversion of GaP QDs occur wide range wavelength (from UV-light to blue light) due to wide absorbance range of GaP QDs.

Comparing to CdSe, CIS QDs color conversion devices conducted various studies, our GaP QDs color conversion devices have some insufficient points. However, the results show that the further studies about GaP QDs are valuable to develop GaP QDs as one of next generation color conversion materials.

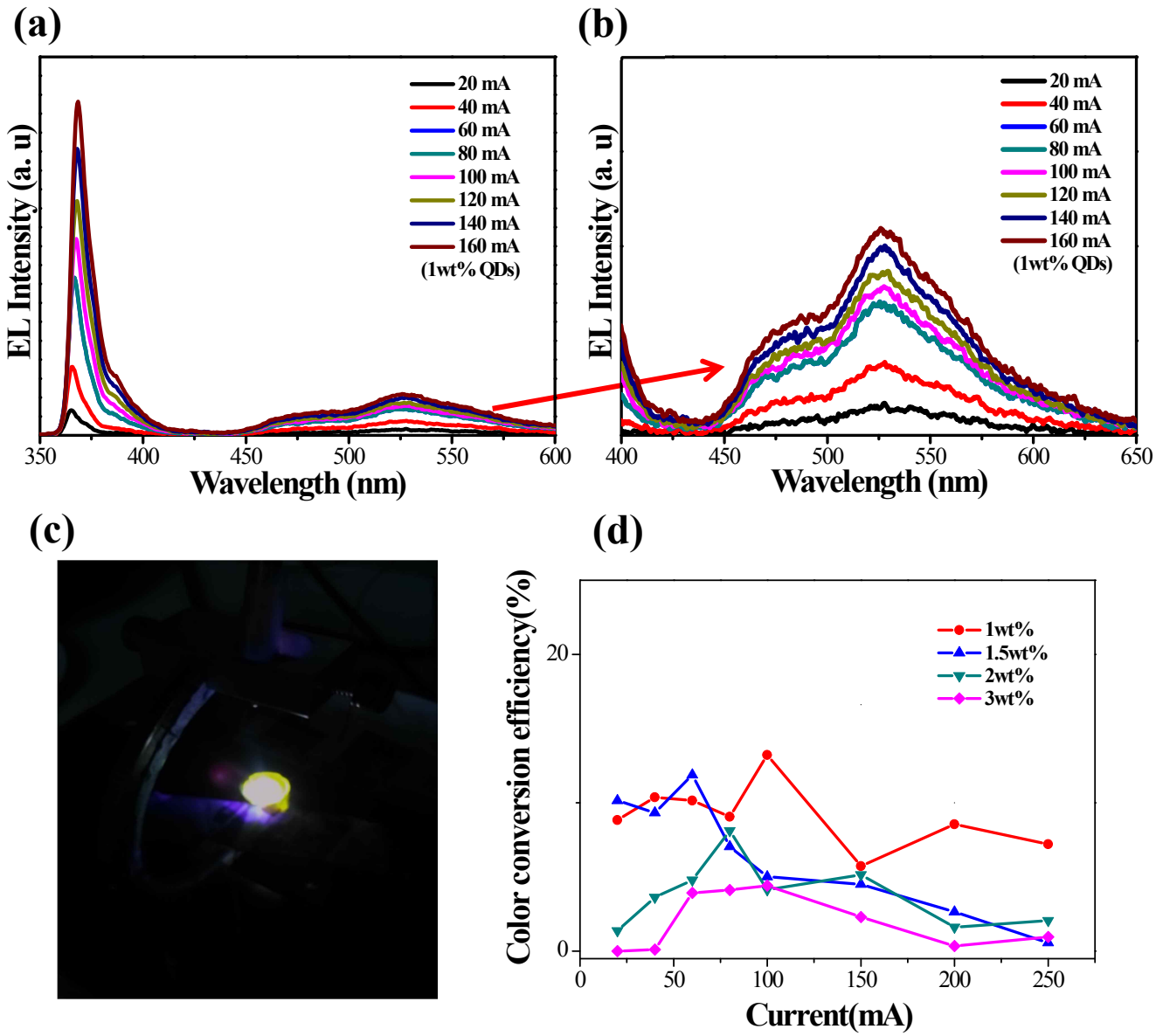

Figure 2.9 (a) Typical EL spectrums, (b) Zoom-in EL spectrums as a function of current, and (c) Photograph under operation of the remote type green GaP QDs color conversion device (1wt% QDs) on UV-LED. (d) Color conversion efficiencies of green GaP QDs color conversion devices on UV-LED as a function of GaP QDs concentration.

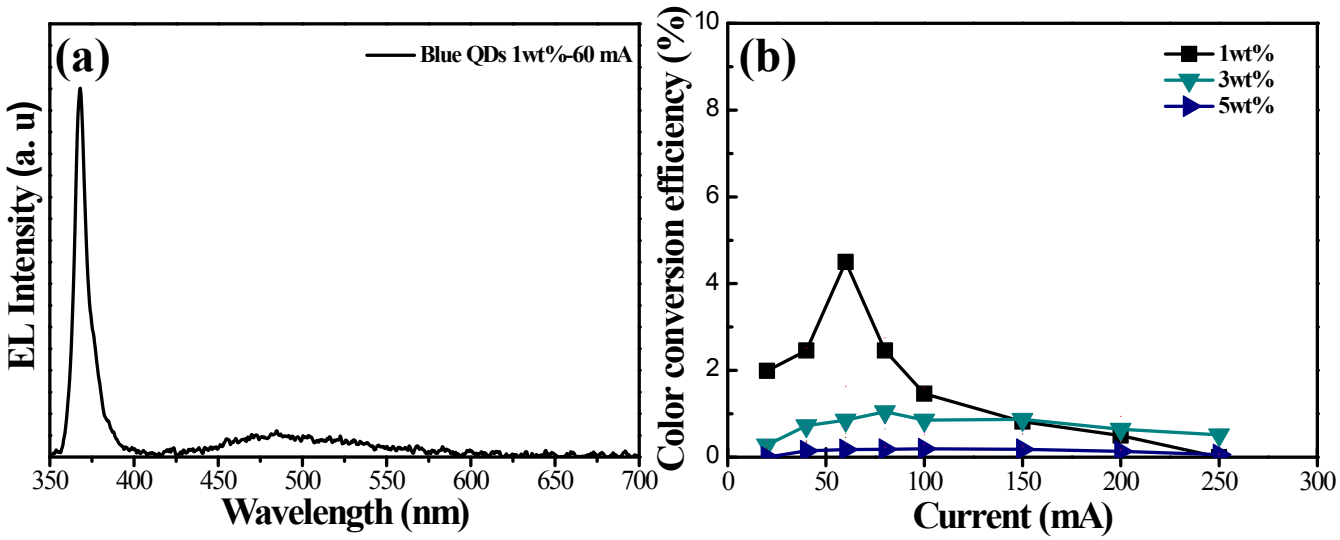

Figure 2.10 (a) Typical EL spectrum of the remote type blue GaP QDs color conversion device (1wt% QDs), (b) Color conversion efficiencies of blue GaP QDs color conversion devices on UV-LED as a function of GaP QDs concentration.

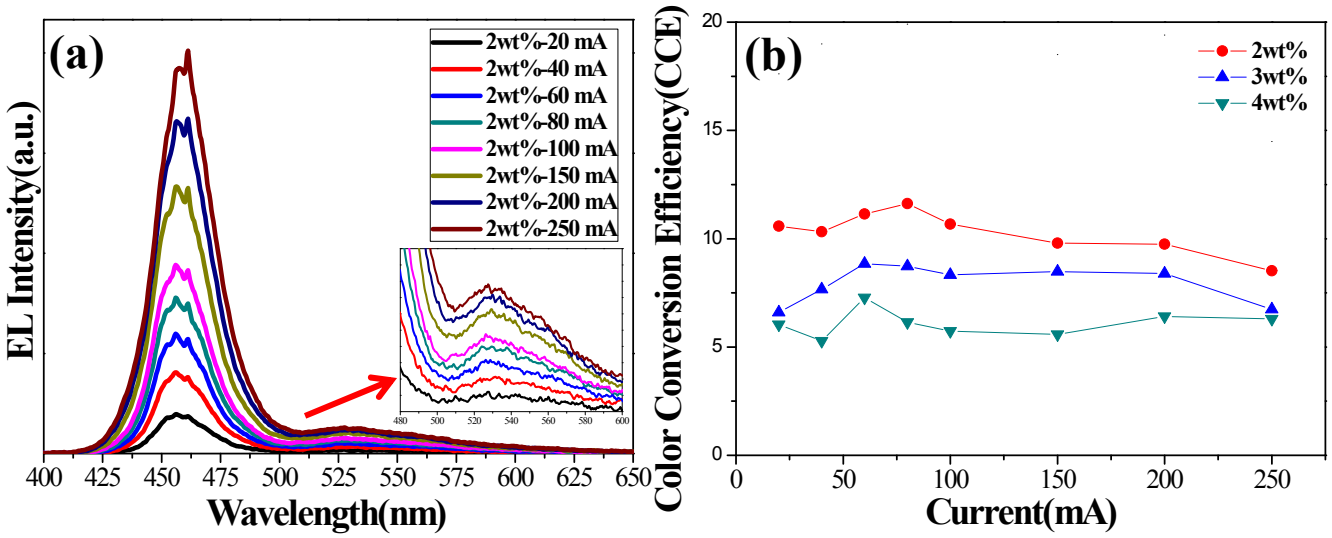

Figure 2.11 (a) Optimized EL spectrum of the remote type green GaP QDs color conversion device (2wt % QDs) with blue LED (b) Color conversion efficiencies of green GaP QDs color conversion devices with blue LED as a function of GaP QDs concentration(1~4wt %)

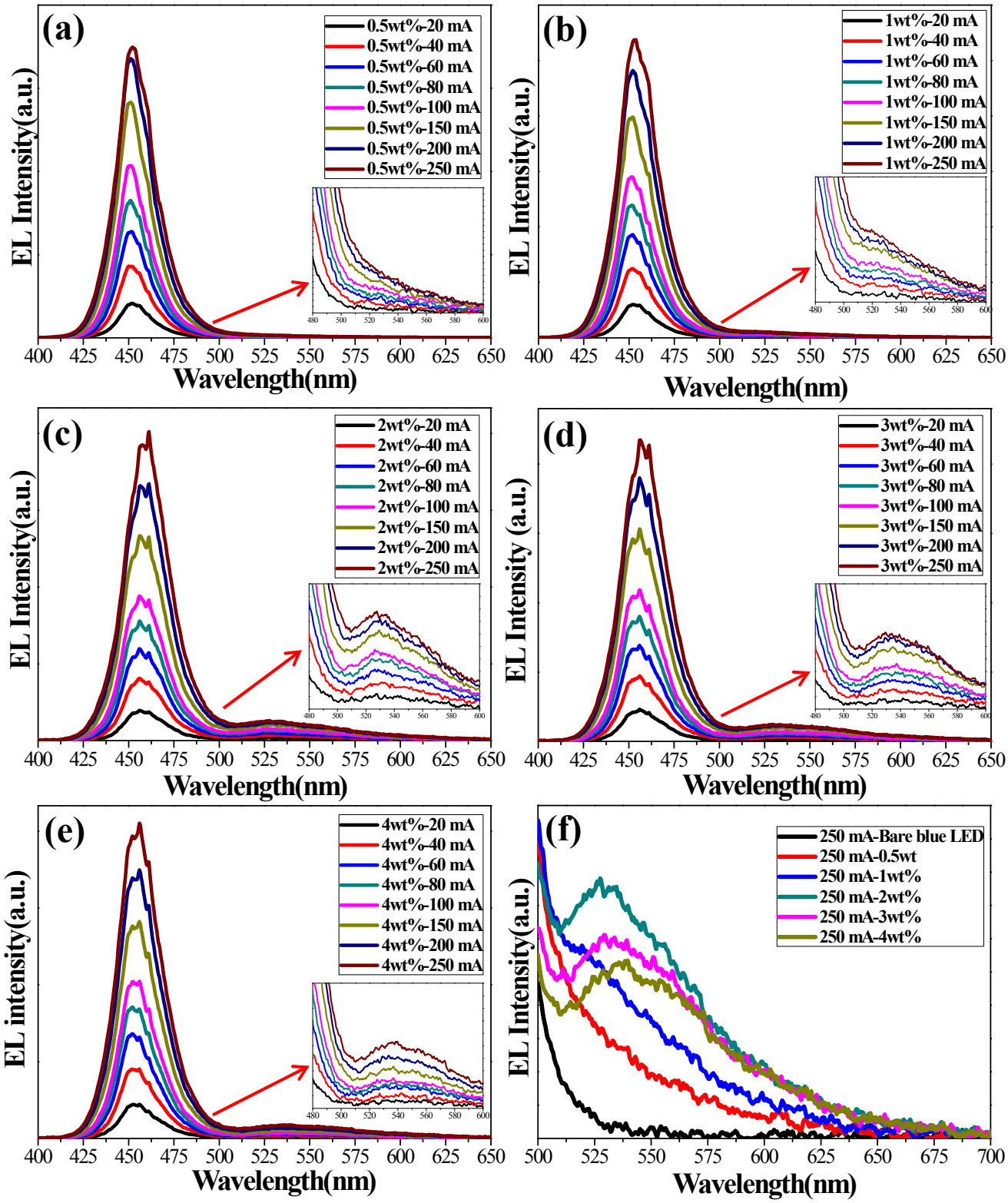

Figure 2.12 (a) ~ (e) EL spectrums with various GaP QDs concentrations (0.5 ~ 4wt %), (f) Zoom in EL spectrums at various GaP QDs concentrations (0 ~ 4wt %) of the remote type green GaP QDs color conversion device with blue LED (forward current: 250 mA)

2.4 conclusions

In summary, colloidal GaP QDs were synthesized by the facile hot injection method. These materials were characterized by XRD, and TEM. From the characterization, the products were confirmed gallium phosphide, and average particle size was 2~3 nm. However, that has limitation about low crystallinity. The Photoluminescence ranges of GaP QDs were controlled from UV emission (400 nm) to green emission (520 nm) by used surfactant amount at GaP QDs synthesis. PL QYs of GaP QDs of 35~40% for green emission and 15~20% for blue emission were obtained through systematically controlling the synthesis condition. Also, colloidal GaP QDs can be synthesized using various fatty acids as the surfactants. These results were first report of GaP QDs with high luminous efficiency for application to the optical device. We confirmed green emitting color conversion with blue LED, and UV-LED through fabrications of GaP QDs color conversion devices at various QD concentrations. The color conversion efficiency of device was optimized about 12~13% at both LED cases. These results suggest that the colloidal GaP QDs have the possibility as color conversion materials.

References

1. Park, J.; Joo, J.; Kwon, S. G.; Jang, Y.; Hyeon, T. Synthesis of monodisperse spherical nanocrystals. *Angewandte Chemie* 2007, 46, 4630-60.
2. Shirasaki, Y.; Supran, G. J.; Bawendi, M. G.; Bulovic, V. Emergence of colloidal quantum-dot light-emitting technologies. *Nat Photonics* 2013, 7, 13-23.
3. Jang, E.; Jun, S.; Jang, H.; Lim, J.; Kim, B.; Kim, Y. White-light-emitting diodes with quantum dot color converters for display backlights. *Advanced materials* 2010, 22, 3076-80.
4. Tang, J.; Sargent, E. H. Infrared colloidal quantum dots for photovoltaics: fundamentals and recent progress. *Advanced materials* 2011, 23, 12-29.
5. Park, J.; An, K.; Hwang, Y.; Park, J. G.; Noh, H. J.; Kim, J. Y.; Park, J. H.; Hwang, N. M.; Hyeon, T. Ultra-large-scale syntheses of monodisperse nanocrystals. *Nature materials* 2004, 3, 891-5.
6. Talapin, D. V.; Yu, H.; Shevchenko, E. V.; Lobo, A.; Murray, C. B. Synthesis of colloidal PbSe/PbS core-shell nanowires and PbS/Au nanowire-nanocrystal heterostructures. *J Phys Chem C* 2007, 111, 14049-14054.
7. Talapin, D. V.; Nelson, J. H.; Shevchenko, E. V.; Aloni, S.; Sadtler, B.; Alivisatos, A. P. Seeded growth of highly luminescent CdSe/CdS nanoheterostructures with rod and tetrapod morphologies. *Nano letters* 2007, 7, 2951-9.
8. Park, J.; Lee, E.; Hwang, N. M.; Kang, M.; Kim, S. C.; Hwang, Y.; Park, J. G.; Noh, H. J.; Kim, J. Y.; Park, J. H.; Hyeon, T. One-nanometer-scale size-controlled synthesis of monodisperse magnetic iron oxide nanoparticles. *Angewandte Chemie* 2005, 44, 2873-7.
9. Anikeeva, P. O.; Halpert, J. E.; Bawendi, M. G.; Bulovic, V. Quantum dot light-emitting devices with electroluminescence tunable over the entire visible spectrum. *Nano letters* 2009, 9, 2532-6.
10. Murray, C. B.; Norris, D. J.; Bawendi, M. G. Synthesis and Characterization of Nearly Monodisperse Cde (E = S, Se, Te) Semiconductor Nanocrystallites. *J Am Chem Soc* 1993, 115, 8706-8715.
11. Dai, Q.; Duty, C. E.; Hu, M. Z. Semiconductor-nanocrystals-based white light-emitting diodes. *Small* 2010, 6, 1577-88.
12. Sun, Q.; Wang, Y. A.; Li, L. S.; Wang, D. Y.; Zhu, T.; Xu, J.; Yang, C. H.; Li, Y. F. Bright, multicoloured light-emitting diodes based on quantum dots. *Nat Photonics* 2007, 1, 717-722.
13. Chen, B.; Zhong, H.; Wang, M.; Liu, R.; Zou, B. Integration of CuInS2-based nanocrystals for high efficiency and high colour rendering white light-emitting diodes. *Nanoscale* 2013, 5, 3514-9.
14. Medintz, I. L.; Uyeda, H. T.; Goldman, E. R.; Mattoussi, H. Quantum dot bioconjugates for imaging, labelling and sensing. *Nature materials* 2005, 4, 435-46.

15. Kim, S.; Fisher, B.; Eisler, H. J.; Bawendi, M. Type-II quantum dots: CdTe/CdSe(core/shell) and CdSe/ZnTe(core/shell) heterostructures. *J Am Chem Soc* 2003, 125, 11466-7.

16. Mews, A.; Eychmuller, A.; Giersig, M.; Schooss, D.; Weller, H. Preparation, Characterization, and Photophysics of the Quantum-Dot Quantum-Well System Cds/Hgs/Cds. *J Phys Chem-Us* 1994, 98, 934-941.

17. Battaglia, D.; Li, J. J.; Wang, Y.; Peng, X. Colloidal two-dimensional systems: CdSe quantum shells and wells. *Angewandte Chemie* 2003, 42, 5035-9.

18. Li, J. J.; Wang, Y. A.; Guo, W.; Keay, J. C.; Mishima, T. D.; Johnson, M. B.; Peng, X. Large-scale synthesis of nearly monodisperse CdSe/CdS core/shell nanocrystals using air-stable reagents via successive ion layer adsorption and reaction. *J Am Chem Soc* 2003, 125, 12567-75.

19. Bae, W. K.; Char, K.; Hur, H.; Lee, S. Single-step synthesis of quantum dots with chemical composition gradients. *Chem Mater* 2008, 20, 531-539.

20. Reiss, P.; Protiere, M.; Li, L. Core/Shell semiconductor nanocrystals. *Small* 2009, 5, 154-68.

21. Xie, R.; Battaglia, D.; Peng, X. Colloidal InP nanocrystals as efficient emitters covering blue to near-infrared. *J Am Chem Soc* 2007, 129, 15432-3.

22. Kim, T.; Kim, S. W.; Kang, M.; Kim, S. W. Large-Scale Synthesis of InPZnS Alloy Quantum Dots with Dodecanethiol as a Composition Controller. *J Phys Chem Lett* 2012, 3, 214-218.

23. Xie, R.; Peng, X. Synthesis of Cu-doped InP nanocrystals (d-dots) with ZnSe diffusion barrier as efficient and color-tunable NIR emitters. *J Am Chem Soc* 2009, 131, 10645-51.

24. Lim, J.; Bae, W. K.; Lee, D.; Nam, M. K.; Jung, J.; Lee, C.; Char, K.; Lee, S. InP@ZnSeS, Core@Composition Gradient Shell Quantum Dots with Enhanced Stability. *Chem Mater* 2011, 23, 4459-4463.

25. Lim, J.; Park, M.; Bae, W. K.; Lee, D.; Lee, S.; Lee, C.; Char, K. Highly efficient cadmium-free quantum dot light-emitting diodes enabled by the direct formation of excitons within InP@ZnSeS quantum dots. *ACS nano* 2013, 7, 9019-26.

26. Lee, S. H.; Lee, K. H.; Jo, J. H.; Park, B.; Kwon, Y.; Jang, H. S.; Yang, H. Remote-type, high-color gamut white light-emitting diode based on InP quantum dot color converters. *Opt Mater Express* 2014, 4, 1297-1302.

27. Chen, B. K.; Zhong, H. Z.; Zhang, W. Q.; Tan, Z. A.; Li, Y. F.; Yu, C. R.; Zhai, T. Y.; Bando, Y. S.; Yang, S. Y.; Zou, B. S. Highly Emissive and Color-Tunable CuInS2-Based Colloidal Semiconductor Nanocrystals: Off-Stoichiometry Effects and Improved Electroluminescence Performance. *Adv Funct Mater* 2012, 22, 2081-2088.

28. Anikeeva, P. O.; Halpert, J. E.; Bawendi, M. G.; Bulovic, V. Electroluminescence from a mixed red-green-blue colloidal quantum dot monolayer. *Nano letters* 2007, 7, 2196-200.

29. Li, Y. Q.; Rizzo, A.; Cingolani, R.; Gigli, G. Bright white-light-emitting device from ternary

nanocrystal composites. *Advanced materials* 2006, 18, 2545-+.

30. Coe-Sullivan, S.; Steckel, J. S.; Woo, W. K.; Bawendi, M. G.; Bulovic, V. Large-area ordered quantum-dot monolayers via phase separation during spin-casting. *Adv Funct Mater* 2005, 15, 1117-1124.

31. Rizzo, A.; Mazzeo, M.; Biasiucci, M.; Cingolani, R.; Gigli, G. White electroluminescence from a microcontact-printing-deposited CdSe/ZnS colloidal quantum-dot monolayer. *Small* 2008, 4, 2143-7.

32. Xie, R. J.; Hirosaki, N.; Kimura, N.; Sakuma, K.; Mitomo, M. 2-phosphor-converted white light-emitting diodes using oxynitride/nitride phosphors. *Appl Phys Lett* 2007, 90.

33. Nizamoglu, S.; Zengin, G.; Demir, H. V. Color-converting combinations of nanocrystal emitters for warm-white light generation with high color rendering index. *Appl Phys Lett* 2008, 92.

34. Woo, H.; Lim, J.; Lee, Y.; Sung, J.; Shin, H.; Oh, J. M.; Choi, M.; Yoon, H.; Bae, W. K.; Char, K. Robust, processable, and bright quantum dot/organosilicate hybrid films with uniform QD distribution based on thiol-containing organosilicate ligands. *J Mater Chem C* 2013, 1, 1983-1989.

35. Jun, S.; Lee, J.; Jang, E. Highly luminescent and photostable quantum dot-silica monolith and its application to light-emitting diodes. *ACS nano* 2013, 7, 1472-7.

36. Song, W. S.; Yang, H. Efficient White-Light-Emitting Diodes Fabricated from Highly Fluorescent Copper Indium Sulfide Core/Shell Quantum Dots. *Chem Mater* 2012, 24, 1961-1967.

37. Park, J.; Kim, S. W. CuInS2/ZnS core/shell quantum dots by cation exchange and their blue-shifted photoluminescence. *J Mater Chem* 2011, 21, 3745-3750.

38. Zhang, J. B.; Sun, W. P.; Yin, L. P.; Miao, X. S.; Zhang, D. L. One-pot synthesis of hydrophilic CuInS2 and CuInS2-ZnS colloidal quantum dots. *J Mater Chem C* 2014, 2, 4812-4817.

39. Sohn, I. S.; Unithrattil, S.; Im, W. B. Stacked Quantum Dot Embedded Silica Film on a Phosphor Plate for Superior Performance of White Light-Emitting Diodes. *Acs Appl Mater Inter* 2014, 6, 5744-5748.

40. Ziegler, J.; Xu, S.; Kucur, E.; Meister, F.; Batentschuk, M.; Gindele, F.; Nann, T. Silica-Coated InP/ZnS Nanocrystals as Converter Material in White LEDs. *Advanced materials* 2008, 20, 4068-+.

41. Ma, W.; Luther, J. M.; Zheng, H.; Wu, Y.; Alivisatos, A. P. Photovoltaic devices employing ternary PbSxSe1-x nanocrystals. *Nano letters* 2009, 9, 1699-703.

42. Zhao, N.; Osedach, T. P.; Chang, L. Y.; Geyer, S. M.; Wanger, D.; Binda, M. T.; Arango, A. C.; Bawendi, M. G.; Bulovic, V. Colloidal PbS quantum dot solar cells with high fill factor. *ACS nano* 2010, 4, 3743-52.

43. Kim, S. W.; Zimmer, J. P.; Ohnishi, S.; Tracy, J. B.; Frangioni, J. V.; Bawendi, M. G. Engineering InAs(x)P(1-x)/InP/ZnSe III-V alloyed core/shell quantum dots for the near-infrared. *J Am*

Chem Soc 2005, 127, 10526-32.

44. Kher, S. S.; Wells, R. L. A Straightforward, New Method for the Synthesis of Nanocrystalline Gaas and Gap. *Chem Mater* 1994, 6, 2056-2062.

45. Aubuchon, S. R.; Mcphail, A. T.; Wells, R. L.; Giambra, J. A.; Bowser, J. R. Preparation, Characterization and Facile Thermolysis of [X2gap(Sime3)2]2 (X = Br, I) and (Cl3ga2p)N - New Precursors to Nanocrystalline Gallium-Phosphide. *Chem Mater* 1994, 6, 82-86.

46. Micic, O. I.; Sprague, J. R.; Curtis, C. J.; Jones, K. M.; Machol, J. L.; Nozik, A. J.; Giessen, H.; Fluegel, B.; Mohs, G.; Peyghambarian, N. Synthesis and Characterization of Inp, Gap, and Gainp2 Quantum Dots. *J Phys Chem-Us* 1995, 99, 7754-7759.

47. Janik, J. F.; Wells, R. L.; Young, V. G.; Rheingold, A. L.; Guzei, I. A. New pnictinogallanes [H2GaE(SiMe3)(2)](3) (E = P, As) - Formation, structural characterization, and thermal decomposition to afford nanocrystalline GaP and GaAs. *J Am Chem Soc* 1998, 120, 532-537.

48. Kim, Y. H.; Jun, Y. W.; Jun, B. H.; Lee, S. M.; Cheon, J. W. Sterically induced shape and crystalline phase control of GaP nanocrystals. *J Am Chem Soc* 2002, 124, 13656-13657.

49. Gao, S. M.; Lu, J.; Zhao, Y.; Chen, N.; Xie, Y. The growth process, stability of GaP nanocrystals and formation of Ga3P nanocrystals under solvothermal conditions in benzene. *Eur J Inorg Chem* 2003, 1822-1827.

50. Gao, S. M.; Lu, J.; Chen, N.; Zhao, Y.; Xie, Y. Aqueous synthesis of III-V semiconductor GaP and InP exhibiting pronounced quantum confinement. *Chem Commun* 2002, 3064-3065.

51. Beberwyck, B. J.; Alivisatos, P. Ion exchange synthesis of III-V nanocrystals. *Abstr Pap Am Chem S* 2013, 245.

52. Lauth, J.; Strupeit, T.; Komowski, A.; Weller, H. A Transmetalation Route for Colloidal GaAs Nanocrystals and Additional III-V Semiconductor Materials. *Chem Mater* 2013, 25, 1377-1383.

53. Kim, S.; Kim, T.; Kang, M.; Kwak, S. K.; Yoo, T. W.; Park, L. S.; Yang, I.; Hwang, S.; Lee, J. E.; Kim, S. K.; Kim, S. W. Highly luminescent InP/GaP/ZnS nanocrystals and their application to white light-emitting diodes. *J Am Chem Soc* 2012, 134, 3804-9.

54. Reiss, P.; Bleuse, J.; Pron, A. Highly luminescent CdSe/ZnSe core/shell nanocrystals of low size dispersion. *Nano letters* 2002, 2, 781-784.

55. Song, W. S.; Yang, H. Fabrication of white light-emitting diodes based on solvothermally synthesized copper indium sulfide quantum dots as color converters. *Appl Phys Lett* 2012, 100.